chemosensors

MDPI

Review

Metal–Organic Frameworks–Based Surface–Enhanced Raman Scattering Substrates for Gas Sensing

Weiqing Xiong, Xiaoyan Wang, Haiquan Liu and Yue Zhang *

Tianjin Key Laboratory of Life and Health Detection, Life and Health Intelligent Research Institute, School of Chemistry & Chemical Engineering, Tianjin University of Technology, Tianjin 300384, China
* Correspondence: yuezhang@tjut.edu.cn

Abstract: Gas sensing holds great significance in environment monitoring, real–time security alerts and clinical diagnosis, which require sensing technology to distinguish various target molecules with extreme sensitivity and selectivity. Surface–enhanced Raman spectroscopy (SERS) has great potential in gas sensing for its single molecule sensitivity and fingerprint specificity. However, different from molecule sensing in solutions, SERS detection of gas often suffers from low sensitivity as gas molecules usually display a low Raman cross–section and poor affinity on traditional noble metal nanoparticle (NMNP)–based substrates. Therefore, much effort has been made to solve these problems. Fortunately, the appearance of metal–organic frameworks (MOFs) has shed new light on this direction. Due to the unique functional characteristics of MOFs, such as controllable pore size/shape, structural diversity and large specific surface area, SERS substrates based on MOFs can achieve high sensitivity, excellent selectivity and good stability. Although several reviews on MOF–based SERS substrates have been reported, few focus on gas sensing, which is a great challenge. Here, we mainly review the latest research progress on SERS substrates based on different MOFs. Sensitive and active SERS substrates can be prepared according to the unique advantages of MOFs with different metal centers. Then, we focus on composite SERS substrates based on different MOFs and NMNPs and summarize the application of composite SERS substrates in gas sensing. Finally, the future difficulties and potential possibilities of SERS substrates based on MOFs and NMNPs for gas sensing are discussed.

Keywords: metal–organic frameworks; noble metal nanoparticles; surface–enhanced Raman spectroscopy; gas sensing

Citation: Xiong, W.; Wang, X.; Liu, H.; Zhang, Y. Metal–Organic Frameworks–Based Surface–Enhanced Raman Scattering Substrates for Gas Sensing. *Chemosensors* **2023**, *11*, 541. https://doi.org/10.3390/chemosensors11100541

Academic Editor: Andrea Ponzoni

Received: 2 September 2023
Revised: 4 October 2023
Accepted: 10 October 2023
Published: 17 October 2023

1. Introduction

For the importance of gas in our daily life, gas detection is crucial in many aspects, for example, environmental monitoring [1,2], food safety [3,4], industrial pollution [5] and healthcare [6,7]. Gas sensors are mainly based on different conversion mechanisms and structures, which can be subdivided into chemical resistance sensors, capacitive/impedance sensors, field effect transistors (FETs), and optical sensors [8]. In comparison to alternative gas sensors, surface–enhanced Raman spectroscopy (SERS) gas sensors present a range of benefits: (1) Remarkable sensitivity: capable of detecting at the level of individual molecules, with signal amplification factors reaching magnitudes of 10^{10} to 10^{14}. (2) Exceptional specificity: SERS enables the acquisition of spectroscopic information that serves as a unique identifier for gas molecules, demonstrating high–resolution and identification capabilities. (3) Rapid response time: SERS facilitates the completion of the detection process within milliseconds or microseconds, making it suitable for gas systems with dynamic changes. (4) Straightforward operation: SERS only necessitates the introduction of the gas sample onto the surface of metal nanostructures to obtain the Raman spectroscopic signal, eliminating the requirement for intricate pretreatment and labeling procedures. Based on these advantages, SERS has emerged as an immensely promising approach for

gas detection [9–11]. SERS is a technique used to identify and quantify analytes by utilizing their distinct molecular vibration fingerprints. Nonetheless, the Raman scattering signals emitted by the majority of gas molecules are generally weak, making them inadequate for meeting the analytical requirements. Thus, designing novel sensing strategies or new substrates is becoming the main focus of research for solving the conundrum.

The generation of Raman scattering in a molecule generally arises from the charge exchange that takes place between the metal substrate and the absorbed target on its surface when exposed to an external electric field. Thus, modulating the charge transfer or increasing the local electric field acting on the molecule can result in enhanced Raman scattered light, which has been recognized as a chemical enhancement mechanism (CM) and electro–magnetic enhancement mechanism (EM) [12–14]. The CM is considered to be induced by three categories of mechanisms: (i) The molecules involved in the process experience an increased polarizability. (ii) Photon excitation promotes the electronic excitation of the molecules. (iii) In certain scenarios, the electronic excitation of a system involves the localization of orbitals in different regions. This results in charge transfer transitions. For instance, an electron initially restricted to a metal orbital is later moved to a molecular orbital confined to the organic molecule [15,16]. When exposed to incident light, a phenomenon known as EM occurs due to the vibration of electrons on the surface of nanostructured metals, typically precious metals like Au, Ag and Cu [17]. The existence of interstitial cavities among adjacent noble metallic nanostructures induces a localized surface plasmon resonance (LSPR) at a specific excitation frequency, resulting in a focused amplification of the local electromagnetic field known as a "hot spot" [18–20]. The strength of SERS is heavily influenced by the presence and quality of these "hot spots". Consequently, the formation of highly intense SERS signals is facilitated by more favorable assembly modes that facilitate the formation of such "hot spots". In the assessment of SERS performance, a crucial parameter to consider is the enhancement factor (EF), which holds significant relevance in analytical chemistry applications, offering an intuitive measure. The enhancement factor (EF) quantifies the extent to which the SERS signal surpasses that of normal Raman spectroscopy under specific experimental conditions. Its primary purpose is to evaluate the effectiveness of SERS performance [21]. The choice of substrate for SERS detection assumes great significance in achieving a satisfactory EF, regardless of whether it involves EM or CM. Thus, numerous researchers have dedicated their efforts to designing and fabricating SERS substrates that can fulfill the requirements of gas sensing applications [22].

During practical gas sensing, the use of current SERS active substrates presents problems such as weak affinity between the plasma surface and the gas molecules, non–differentiated target concentration/enrichment, and substantial molecular interference. Research has found that integrating plasma nanostructures/Nanoparticles (NPs) with metal–organic frameworks (MOFs) has many inherent advantages in SERS detection [23], such as the efficient enrichment and selective capture of trace analytes with high mobility in complex matrices [24]. Therefore, in the presence of precious metals, the introduction of MOFs to fabricate composite substrate is an effective solution to overcome the current SERS bottleneck.

MOFs, which are fascinating porous crystalline materials, are formed through the interconnection of inorganic nodes by organic spokes. They exhibit structural features such as elevated porosity, considerable specific surface area, and modifiable arrangement, all of which make MOFs excellent options for SERS substrate design and gas sensing [25]. Primarily, the intrinsic porosity of MOFs provides a substantial rise in specific surface area and potential active sites. These active sites include unsaturated open metal sites for coordination as well as termination functional groups. This unique characteristic facilitates enhanced gas absorption and transportation capabilities [26]. One crucial function of MOFs is their capability to preconcentrate the target analyte, thereby enhancing sensitivity. Another important aspect lies in their ability to selectively adsorb specific analytes. This selectivity is achieved through the customization of pore dimensions/structure and the

physicochemical surroundings of the MOFs, including factors such as acidity/alkalinity, hydrophilicity/hydrophobicity, and electron–rich/electron–deficient characteristics. The enhanced selectivity and sensitivity resulting from this selective adsorption significantly improve overall performance [27]. Furthermore, the highly organized crystalline structure and predictable arrangement of atoms and molecules in MOFs enable precise structural recognition and correlation of properties at the atomic and molecular level. This is especially evident in the context of host–guest interactions [28,29]. Fourth, in addition to some cases involving enhanced adsorption and redox reactions, the reversible absorption and release of gases by MOFs contribute to good reproducibility of the sensors [30]. Fifth, the relatively high thermal and chemical stability of most MOFs ensures the long life of MOF–based sensors. In conclusion, MOFs demonstrate captivating properties that make them highly promising for gas sensing applications, particularly when combined with SERS technology [31].

With the design and synthesis of the SERS platform based on MOFs, benefits and possibilities are becoming increasingly apparent. In the most recent times, several reviews have summarized the SERS substrates based on MOFs [32–35], but few of them focus on gas sensing, which is of great challenges. So, in this article, we first briefly introduce the latest progress using single–component MOFs, two–component material (MOFs and noble metal nanoparticles (NMNPs) with different metal centers) and three–component material (MOFs and two other components) as SERS substrates [36–38]. Then, we focus on summarizing the research progress of these MOF–based SERS substrates for gas sensing. In conclusion, the difficulties and prospects for the prospective advancement of MOF–based SERS substrates and gas sensing are featured.

2. One–Component SERS Substrate: MOFs

With their extensive specific surface region, porous structure, and versatility, MOFs significantly contribute to augmenting the interaction between gas molecules and solid metal surfaces. This pivotal role ensures enhanced contact between the two entities. The tremendous transformative capacity and exemplary restoration performance of MOFs themselves make them ideal candidates for SERS active substrates, as they not only have easy access compared to metal nanostructures coated with MOFs but also have extended sensing capabilities, such as stable photoinduced vacancy defects, high customization and rich active site. The utilization of single–component MOF substrates holds the potential to transform non–SERS active substrates into SERS active substrates. Consequently, the exploration of single MOF substrates exhibiting robust SERS signal enhancement is an exceptionally promising avenue. Furthermore, the pore diameter and surface characteristics of MOFs can be readily manipulated through the selection of precursors and adjusting synthetic conditions. The meticulous control mentioned above empowers the precise adjustment of MOFs' chemical selectivity, thereby facilitating the utilization of various mechanisms such as molecular sieving, π–π stacking, hydrogen bonding, electrostatic interactions and more. As a result, MOFs demonstrate immense potential in the field of analytical chemistry.

2.1. Ti–MOFs

Under light excitation, MOFs undergo electron–hole separation and oxygen vacancy defects may be caused by bond breakage between reducing metal sites and oxygen atoms, which is called photo–induced oxygen defects (PIVO). The presence of PIVO in MOFs can alter the electronic energy state of charge transfer on the substrate surface, which helps to improve the sensitivity of SERS detection. Zhao et al. [39] synthesized Ti–MOFs with PIVO properties (referred to as D–MIL–NH_2) in a 0.01 M triethanolamine (TEOA) solution under a nitrogen gas atmosphere at a temperature of 298.15 K using a 500 W Xe lamp. For comparison, they also prepared nearly defect–free MIL125 (Ti)–NH_2 (referred to as MIL–125–NH_2). The results indicated that D–MIL–125–NH_2 exhibited significant stability for at least two weeks when exposed to ambient atmosphere. The stability can be attributed

to the combined influence of steric hindrance and electron delocalization surrounding vacancy defects, working in synergy (Figure 1). Consequently, the researchers achieved a significantly enhanced SERS effect, outperforming that of original MOFs. This enhancement was accompanied by a substantial three–order reduction in the limit of detection.

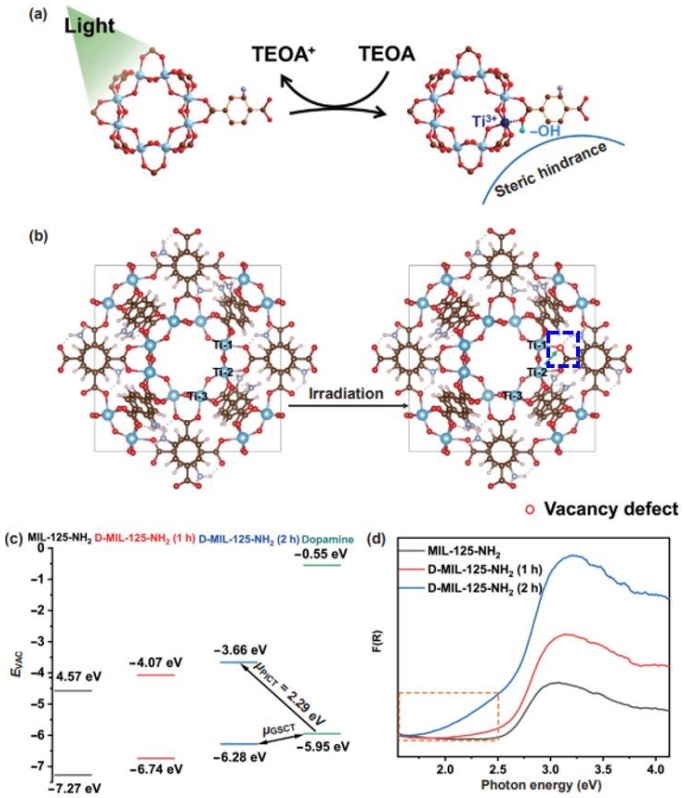

Figure 1. (**a**) Illustration of steric hindrance in D–MIL–125–NH_2 as a result of coordination between dangling groups of –OH and an adjacent metal center (Ti). (**b**) Comparative evaluation of the charge calculated on Ti sites surrounding oxygen vacancy defects in D–MIL–125–NH_2 in contrast to those in the pristine MIL–125–NH_2. (**c**) Diagram depicting the energy band positions of dopamine on MIL–125–NH_2, D–MIL–125–NH_2 (1 h), and D–MIL–125–NH_2 (2 h) relative to the vacuum level for the purpose of comparing their charge–transfer pathways. (**d**) UV–Vis diffuse reflectance spectra of MIL–125–NH_2, D–MIL–125–NH_2 (1 h), and D–MIL–125–NH_2 (2 h) [39].

2.2. Co–MOFs

A significant structural feature of MOFs, namely its high customizability, contributes to the selectivity of SERS. By thoughtful manipulation of the metal cores, organic linkers, and framework architectures of MOF–based SERS substrates, it becomes viable to intentionally transform the electronic band structures of the substrates. This targeted manipulation allows for aligning the electronic band structures with those of the specific analyte being targeted, leading to the distinct detection of different species. For example, Sun et al. [40] synthesized Co–MOFs (including ZIF–67, Co–MOF–74, and Co–TCPP), using various organic ligands. They demonstrated that by manipulating the metal centers, organic ligands, and framework topology of MOF–based SERS substrates, it is feasible to selectively tune the electronic band structure of the MOF matrix to match the electronic band structure of the target analytes, leading to the generation of distinct observable species. Notably, the SERS EF of MOF–based SERS substrates can be significantly enhanced to 10^6, with detection limits as low as 10^{-8} M. By optimizing the pore structure and modifying the surface, the EF of MOF–based SERS substrates is comparable to that of noble metals without the presence of "hots pots" and recently reported semiconductors. This selective enhancement is attributed to the controlled combination of various resonances such as charge transfer,

interband resonance, molecular resonance, and ground–state charge transfer interactions (as illustrated in Figure 2).

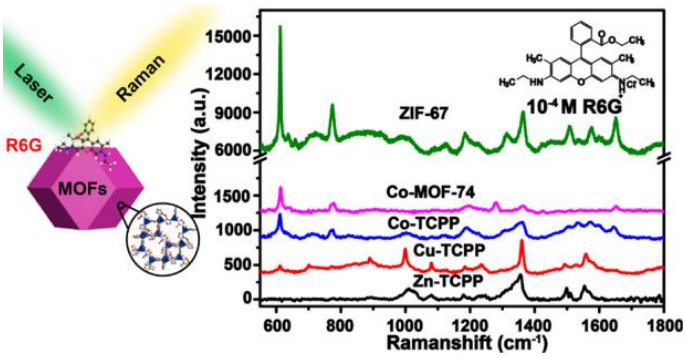

Figure 2. Raman spectra of R6G detection using MOFs with different metal centers as SERS substrate [40].

2.3. Fe–MOFs

MIL–100 (Fe) is an excellent adsorbent with Fe^{3+} as the metal center and pyromellitic acid as the organic ligand. It has high hydrothermal stability and non–toxic characteristics. Both metal ions and oxygen groups in MOFs can be used as "active sites" for effectively binding polar organic molecules. Utilizing a high–temperature hydrothermal method, Fu et al. [41] successfully synthesized MIL–100 (Fe), a MOF characterized by an aromatic ligand structure and metallic active sites. As a result, volatile organic compounds (VOCs) exhibit a strong preference for adsorbing into the structure of MIL–100 (Fe) because of the existence of aromatic ligands and the coordination interactions facilitated by Fe–heteroatomic bonds (as verified by specific theoretical calculations shown in Figure 3). This distinctive adsorption behavior, primarily mediated by π–π interactions, makes MIL–100 (Fe) an exceptional SERS active substrate which is able to efficiently detect a broad range of small organic compounds, including toluene, chloroform and acetone, with remarkable sensitivity.

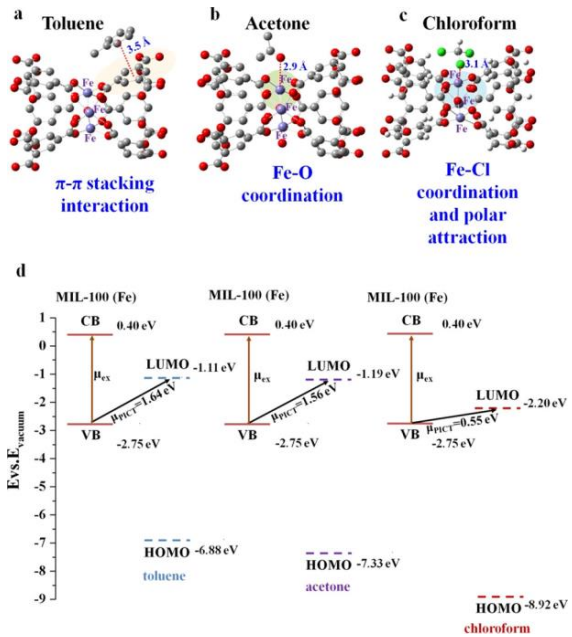

Figure 3. Affinity for adsorption and bonding strength of three VOC molecules on MIL–100 (Fe): (**a**) toluene, (**b**) acetone, and (**c**) chloroform (Fe shown in purple, C in brown, O in red, and Cl in green). (**d**) Energy–level charts representing the positions of toluene, acetone, and chloroform in relation to MIL–100 (Fe), with respect to the vacuum level [41].

2.4. Mo–MOFs

Polyoxometalates (POMs) have been used for electrochemistry, adsorption, photochromism, catalysis, and magnetism due to their unique structures. As a subset of metal oxides, POM has a variety of types, structures and sizes. Mo–MOFs consist of molybdenum trioxide and imidazole to form octal molybdate, in which Mo is +6 valence, which is very easily reduced to +5 valence and has excellent photocatalytic activity. Mixed valence MOFs are advantageous for charge transfer transitions and play a vital role in enhancing the SERS characteristics of MOFs. A Mo–based MOF substrate with remarkable SERS activity was successfully synthesized by Chen et al. [42] through a straightforward solvothermal method conducted at low temperatures. The substrate exhibited high SERS activity as a result of the formation of mixed valence Mo–O clusters induced by ultraviolet (UV) irradiation. The presence of oxygen vacancies in UV Mo–MOFs enhances the efficient exchange of charges between the substrate and the adsorbed molecule. This, as a result, triggers the creation of active SERS sites. The porous architecture and significant surface area of Mo–MOFs facilitate the adsorption and anchoring of SERS molecular probes, resulting in further enhancement of the SERS signal (Figure 4).

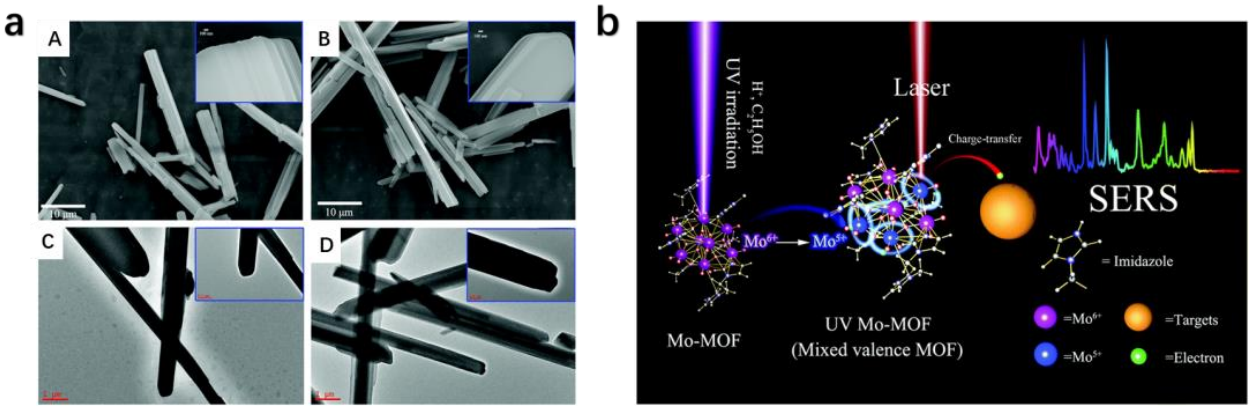

Figure 4. (**a**) SEM (**a-A**,**B**) and TEM (**a-C**,**D**) images of the Mo–MOF (**a-A**,**C**) and the UV Mo–MOF (**a-B**,**D**). (**b**) The SERS effect of the UV Mo–MOFs [42].

3. Two–Component SERS Substrate: MOFs/NMNPs

Numerous studies have consistently demonstrated that EM enhancement exhibits superior performance in practical applications compared to CM enhancement. As a result, the focus of extensive research has been on traditional plasmonic metal particles, such as NMNPs, due to their remarkable LSPR characteristics, which contribute to high EF in SERS detection. However, the tendency of colloidal NMNPs to form clusters and their uneven dispersion on substrates often diminishes sensitivity and reproducibility. Furthermore, prolonged exposure of NMNPs to the surrounding environment leads to contamination or oxidation, negatively impacting their selectivity for target molecules. These aforementioned limitations severely impede the practical implementation and further advancement of SERS technology.

MOFs are highly regarded in the field of SERS sensing as a result of their outstanding pre–concentration capability and molecular sieve–like protection. These unique characteristics have led to their extensive application, enabling them to enhance the amount of target molecules absorbed per unit and selectively filter out specific molecules from complex matrix environments [43]. Moreover, apart from the EM enhancement achieved by using NMNPs, certain MOFs can also facilitate interfacial charge transfer between small molecules. This charge transfer arises from the CM mechanism of MOFs and offers superior selectivity compared to EM enhancement for target molecules. Therefore, by combining the excellent LSPR properties of NMNPs with the CT characteristics of MOFs, structure engineering strategies can create a heterogeneous SERS platform that synergistically enhances sensitivity and showcases superior selectivity for target analytes [44].

3.1. Zn–MOFs/NMNPs

Zn–MOFs are composed of zinc ions interconnected with imidazolium, which have the advantages of being mild, easy to control and have good stability. Using the advantages of zeolitic imidazolate framework–8 (ZIF–8), Wang et al. [45] demonstrated a reliable SERS strategy using ZIF–8 coated ordered gold superparticles (GSPs@ZIF–8) as a substrate for gaseous aldehydes' detection. Initially, GSPs were produced using an adapted oil–in–water (O/W) microemulsion assembly technique, resulting in the formation of GSPs with an average size of 170 ± 30 nm. Subsequently, a ZIF–8 shell, approximately 150 nm in thickness, was uniformly coated around each individual GSP core, referred to as GSPs@ZIF–8. To maintain the super–lattice structure of the GSPs and retain their porous nature, the construction of the ZIF–8 shell was carried out using a comparatively gentle method. Within the core–shell 3D structure, the GSPs functioned as SERS hotspots, effectively enhancing the EM field. Simultaneously, the ZIF–8 shell layer has multiple functions. Firstly, it protects GSPs from being affected by external factors and prevents their aggregation, thus maintaining their dispersion state. Secondly, the ZIF–8 shell layer reduces the flow velocity of gas biomarkers on the surface, which helps to increase the contact time with GSPs. Lastly, the ZIF–8 shell layer can slow down the rapid decline of the electromagnetic field around the GSP surface, further enhancing the stability of the SERS effect (Figure 5a). Thus, the substrate can obtain a much higher sensitivity for the detection of VOCs. In the subsequent work, Wang et al. [46] continuously improved the sensing strategy by using hollow structures of ZIF–8 coated on GSPs (GSPs@H–ZIF–8) (Figure 5b). The newly developed GSPs@H–ZIF–8 substrate not only preserves the high sensitivity observed in the GSPs@ZIF–8–based substrate, but also provides additional space for selective absorption of target molecules. This gap space effectively diminishes Raman signal interference originating from non–target molecules in SERS spectra, thereby enhancing the reliability of the results. Notably, the limit of detection for GSPs@H–ZIF–8 was 21.2 ppb, which still fulfilled the detectability requirements for 4–ethylbenzaldehyde, whereas the detection limit of GSPs@ZIF–8 decreased to 138 ppb.

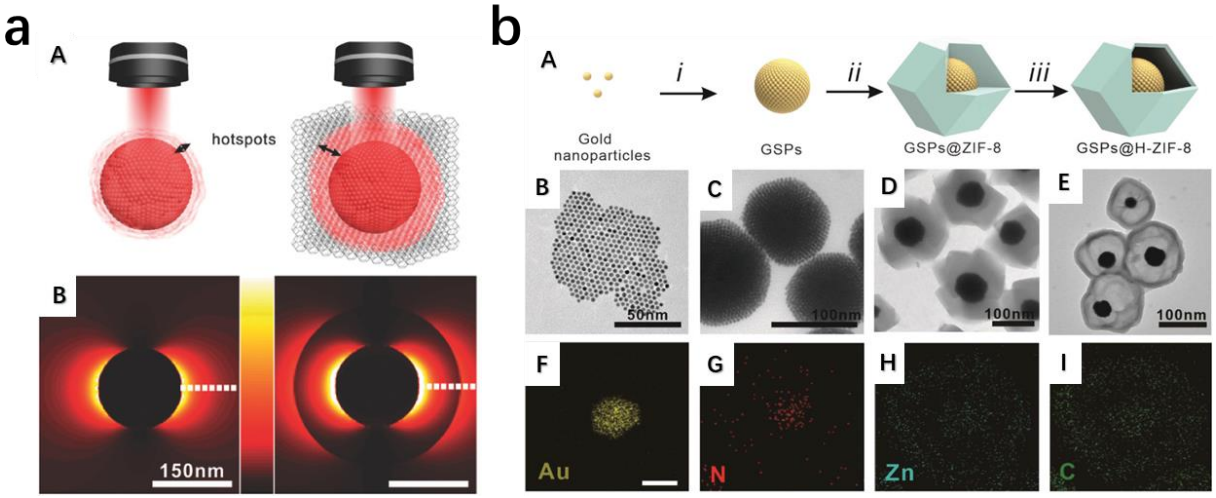

Figure 5. (**a**) (**a-A**) Hotspots of the GSP and GSP@ZIF–8, (**a-B**) 2D FDTD simulations of a GSP and the GSP@ZIF–8 [45]. (**b**) (**b-A**) The preparation process of GSPs@H–ZIF–8, (i) gold nanoparticles assembled into GSPs, (ii) ZIF–8 coated on GSPs surface, (iii) etched hol–low–structured ZIF–8 on GSPs (GSPs@H–ZIF–8). (**b-F**–**I**) EDS analysis, and TEM images of (**b-B**) GNPs, (**b-C**) GSPs, (**b-D**) GSPs@ZIF–8, and (**b-E**) GSPs@H–ZIF–8 [46].

Recently, a noteworthy phenomenon known as plasmon–driven surface catalysis (PDSC) has emerged in the context of SERS. This phenomenon occurs at the interface between the metal and the surrounding medium, where it can modify the optical and electrical properties of the medium. Consequently, it assists in the application of heteroge-

neous catalysis in various domains, including SERS sensing. Huang et al. [47] conducted a study on PDSC reactions within the plasmonic MOF interface of Ag NP@ZIF–8 (Figure 6), involving the conversion of p–aminothiopheno (PATP) to 4,4′–dimercaptoazobenzene (trans–DMAB). The researchers observed reversible PDSC reactions at the Ag NP/ZIF–8 interface in a water–based context. These reactions were found to be modulated by the presence of a reducing agent ($NaBH_4$) or an oxidizing agent (H_2O_2), as confirmed by on–site monitoring of SERS spectra. Furthermore, the Ag NP@ZIF–8 nanostructures exhibited remarkable stability against oxidation etching by H_2O_2, owing to the protective ZIF–8 shell. Surprisingly, in an airy atmosphere, the PDSC reactions were solely detected at the interface of Ag NP/ZIF–8 with a diminished SERS enhancement in comparison to pure Ag NPs.

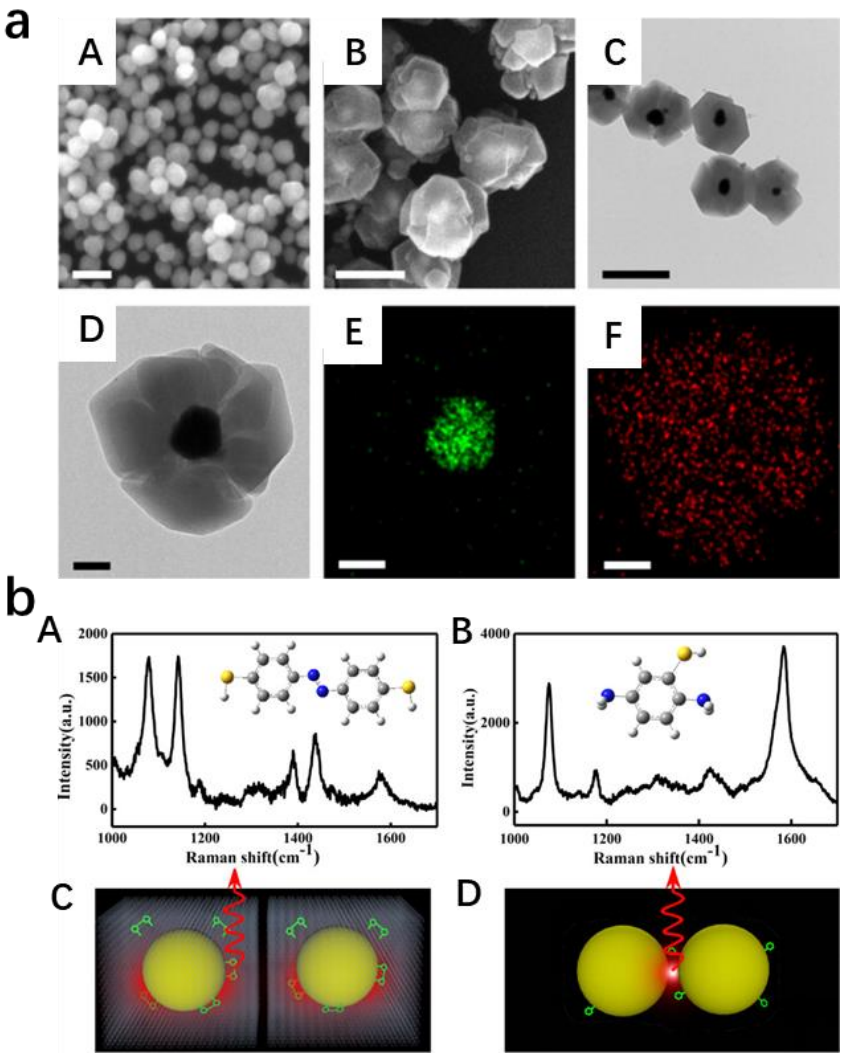

Figure 6. (**a**) SEM images of fabricated Ag NPs (**a-A**) (scale bar: 200 nm) and AgNP@ZIF–8 composites (**a-B**) (scale bar: 500 nm). (**a-C**) TEM images of AgNP@ZIF–8 composites. Scale bar: 500 nm. (**a-D**) Magnified TEM image of individual AgNP@ZIF–8 nanoparticles, along with the elemental mapping of Ag (**a-E**) and Zn (**a-F**). Scale bar: 100 nm. (**b**) (**b-A**) SERS spectra of gas–phase PATP molecules tested on AgNP@ZIF–8 and (**b-B**) bare Ag NPs as SERS substrates. (**b-C**) Schematic representation of trans–catalysis of DMAB by gas–phase PATP molecules adsorbed on AgNP@ZIF–8. (**b-D**) Schematic representation of uncatalyzed reaction of PATP gas molecules adsorbed on Ag NPs [47].

SERS can achieve single molecule–level detection by capturing the molecule within highly sensitive "hot spots", typically found at the microscopic crevices between adjoining

silver (Ag) or gold (Au) nanostructures. However, only a small fraction, less than 1%, of the molecules situated at these hot spots account for approximately 70% of the total SERS intensity. This significant variation in SERS contribution among analyte molecules at different locations ultimately leads to limited quantification capability. To enhance the quantification capability, Yang et al. [48] implemented a novel approach by preventing the formation of highly sensitive SERS sites. They accomplished this by incorporating a dense MOF coating as a protective layer, impeding the close proximity and clustering of gold nanorods (AuNRs) (Figure 7). Despite the decreased sensitivity caused by the existence of these highly sensitive SERS hotspots, the sleek surface of the polydimethylsiloxane (PDMS) brush counterbalances the loss of these regions by spreading the analyte across a significantly larger surface area, which subsequently undergoes a million–fold concentration following solvent evaporation. The porous MOF coating surrounding the Au nanorods selectively allowed only analytes smaller than the pore size to approach and contribute to the SERS spectrum. Consequently, this simplified the SERS spectrum, enabling robust identification of the analytes in complex samples. Notably, the method enabled specific identification of 4–nitrobenzenethiol (4–NBT) at nanomolar concentrations in whole blood samples.

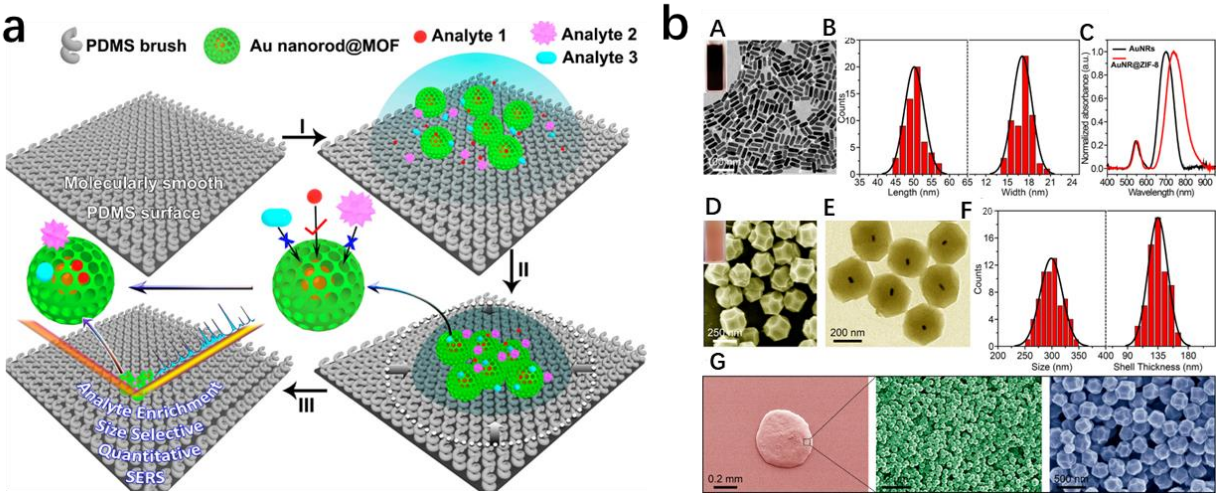

Figure 7. (**a**) Schematic of the working principle of the SERS platform. Process I: applying the liquid sample and Au NR@MOF particles onto the PDMS brush surface. Process II: analyte molecules and the Au NR@MOF particles are concentrated during solvent evaporation. Only those analyte molecules smaller than the aperture size of the MOF shell acting as an analyte filter can pass through, reach the inside Au nanorod, and contribute to the SERS spectrum. Process III: analyte molecules and Au NR@MOF particles form a tiny aggregate after the solvent completely evaporates. (**b**) (**b-A**) SEM depiction of the AuNRs. (**b-B**) Statistical analysis of the length (50.20 ± 2.72 nm) and width (17.07 ± 1.36 nm) distribution of the AuNRs. (**b-C**) UV–vis absorption spectra of the AuNRs and AuNR@ZIF–8 truncated rhombic dodecahedron colloid (TRD). (**b-D**) SEM image illustrating the presence of AuNR@ZIF–8 TRD. (**b-E**) TEM image showcasing the AuNR@ZIF–8 TRDs. (**b-F**) Quantitative assessment of the size (298.93 ± 20.66 nm) and shell thickness (134.95 ± 14.57 nm) distribution for the AuNR@ZIF–8 TRDs. (**b-G**) Formation of an aggregate of AuNR@ZIF–8 TRDs on the surface of the PDMS brush [48].

The generation of SERS signals mainly relies on the presence of electromagnetic hot spots located on plasmonic nanocrystals. To fully exploit the capabilities of hybrid structures incorporating plasmonic nanocrystals and MOFs, Yang et al. [49] employed a straightforward wet–chemistry method to selectively deposit MOFs specifically at the hot spots of metal nanocrystals. ZIF–8 was carefully applied at the tips, middle section, and throughout the entire exterior of the asymmetrical Au nano bipyramids (NBPs) and Au NRs (Figure 8). Nanometer–scale structures derived from NBP and NRs were formed, in which ZIF–8 was selectively deposited at the waist (Au NBP@waist–ZIF) or at the end

(Au NBP@end–ZIF). Among them, Au NBP@end–ZIF demonstrated the optimal SERS functionality. This can be attributed to the concentration augmentation at the hotspots and the substantial field amplification at the tips facilitated by ZIF–8. Therefore, the SERS performance for detecting aniline and toluene can be significantly enhanced.

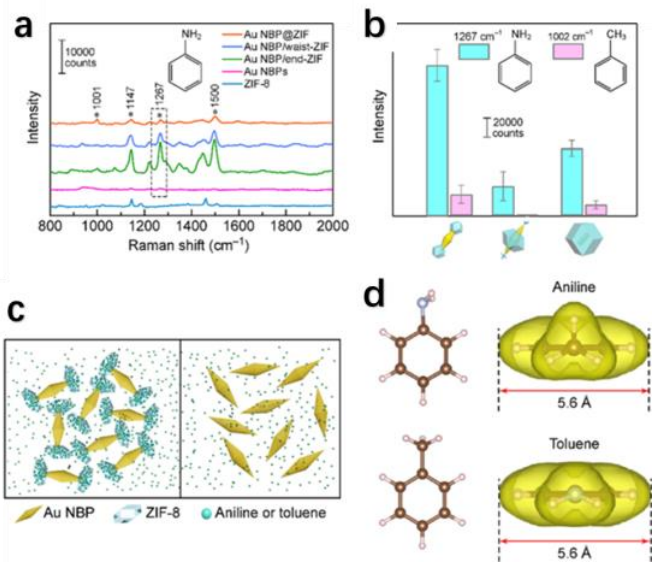

Figure 8. (**a**) SERS spectra acquired using the ZIF–8 nanocrystals, Au NBPs, and NBP/end–ZIF, NBP/waist–ZIF, and NBP@ZIF nanostructures, for the purpose of detecting aniline. (**b**) Mean integrated intensities of the SERS peaks corresponding to aniline and toluene on the various nanostructures. The averaged value for each sample was derived from six Raman spectra obtained from different positions on the substrate. (**c**) Diagrammatic representation demonstrating the adsorption and concentration of analytes in the vapor phase by ZIF–8 at the tips of the Au NBPs. (**d**) Molecular structures and computed kinetic diameters of aniline and toluene [49].

3.2. Co–MOFs/NMNPs

Co–MOFs are synthesized using cobalt as the metal center and 2–methylimidazole and other organic ligands as the linkers. ZIF–67 is one type of water–soluble microporous Co–MOF that can be easily synthesized at room temperature and is often compared to the insoluble ZIF–8. To investigate the CT process and synergistic effects of the ZIF shell and the Au nanostructures, Zhang et al. [50] primarily prepared Au NBP@ZIF–67 and AuNBP@ZIF–8. They then carefully controlled the longitudinal LSPR peak positions of these compounds at 785, 782 and 750 nm using a seed–mediated approach. As a result, six different products were obtained, namely NBP–785@ZIF–8, NBP–785@ZIF–67, NBP–782@ZIF–8, NBP–782@ZIF–67, NBP–750@ZIF–8 and NBP–750@ZIF–67.By altering the thickness and composition of the core–shell design, a cooperative effect was established, verifying that the SERS signals of the target molecules adsorbed on the ZIF shell surface were intensified not only through EM or CT processes but also through their interactions. Since the EM and CT processes were to some extent dependent on the distribution of molecules, they could impact the SERS performance of the substrate. Therefore, Zhang et al. also used the penetrant molecule methyl orange (MO) as a Raman probe and observed reorientation phenomena in Au NBP@ZIF–8 and Au NBP@ZIF–67 (reorientation was defined as the rotation of probe molecules limited by the substrate during the process of adsorption), with the two molecules reorienting in opposite directions (Figure 9).

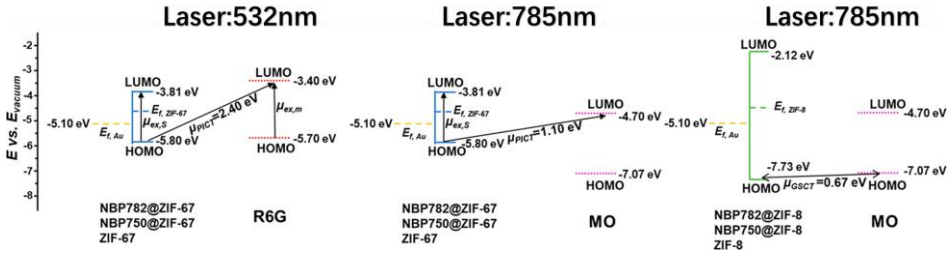

Figure 9. Energy–band plots of the fabricated substrates (NBP@ZIF–67 and NBP@ZIF–8) and the utilized probes (R6G and MO), along with the potential CT under the illumination of 785 and 532 nm lasers [50].

Inspired by hydrophobic fish scales and lotus leaves, Wang et al. [51] designed a reusable and self–cleaning SERS substrate called CC–L–MOF@F–Ag. CC–L–MOF@F–Ag was synthesized in situ at room temperature by using flexible carbon cloth as the supporting material to form multi–layered two–dimensional (2D) Co–MOFs (CC–L–MOFs). Subsequently, the flower–shaped Ag NPs were loaded onto the surface of CC–L–MOFs using electrodeposition techniques (this method allowed for the uniform dispersion of the flower–shaped Ag NPs, reducing the occurrence of aggregation phenomenon) (Figure 10a) followed by chemical modification of the substrate to achieve superhydrophobicity. The Ag NPs offered numerous pointed edges and tips, generating intense electromagnetic fields known as SERS–active "hot spots" on the substrate. The superhydrophobic nature of the substrate further concentrated the sparsely distributed target molecules and significantly enhanced the SERS intensity.

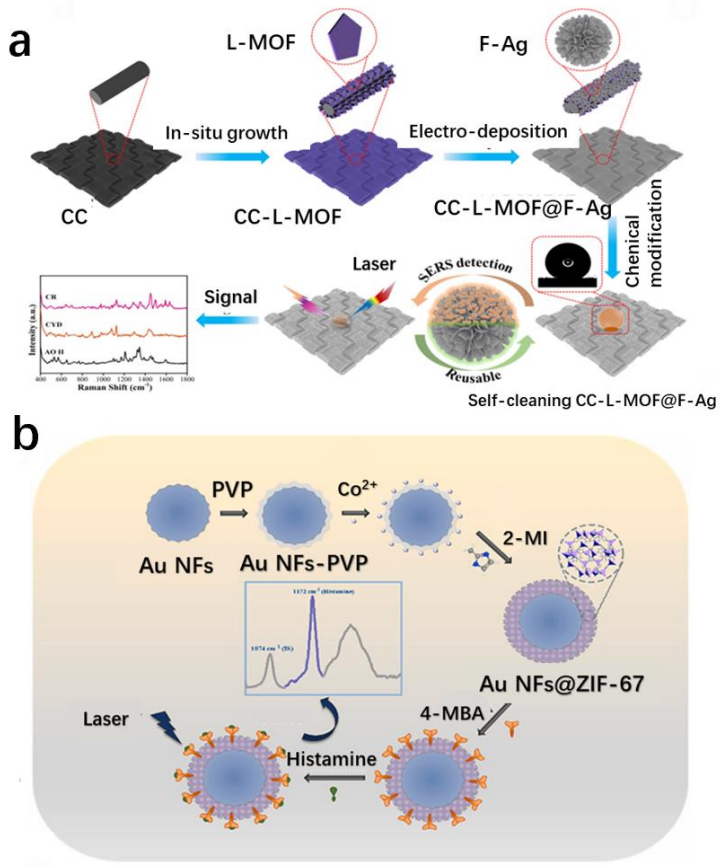

Figure 10. (**a**) Schematic representation of the preparation process of CC–L–MOF@F–Ag and its application in SERS [51]. (**b**) Illustration depicting the SERS sensing platform using MOFs for histamine detection [52].

To achieve quantitative SERS detection in complex matrices and environments, Wang et al. [52] developed a core–shell SERS platform called Au NFs@ZIF–67. The substrate was first synthesized using a reduction method to produce highly branched Au nanoflowers (NFs) (which primarily provide sensitive fingerprints through EM). Subsequently, a wet chemical method was employed to encapsulate the Au NFs within ZIF–67, resulting in a stable core–shell framework (Figure 10b). The morphology of this core–shell structure was controlled by the concentration of the end–capping agent polyvinylpyrrolidone (PVP) and the precursor cobalt ions of MOFs. Furthermore, they preconnected 4–aminobenzaldehyde (4–MBA) as a binding molecule and Raman reference compound to detect histamine and compensate for disparities in histamine signals, allowing for quantitative analysis of histamine using SERS.

3.3. Zr–MOFs/NMNPs

Zr–MOFs are a type of MOF with zirconium as the metal center and terephthalic acid, trimesic acid or multiple functional groups as ligands. Following the theory of hard and soft acids and bases, Zr–MOFs form stronger coordination bonds between high–valence metal ions (Zr^{4+}) and carboxylic acid ligands compared to lower–valence metal ions. As a result, Zr–MOFs not only possess the adsorption capabilities commonly found in MOFs but also exhibit high stability, making them suitable for applications in slightly complex environments to enhance the stability of SERS substrates. In order to improve the efficiency of recovering di(2–ethylhexyl) phthalate (DEHP) from actual plastics, Cai et al. [53] synthesized octahedral–shaped UIO–66 through a high–temperature, high–pressure hydrothermal reaction. They then used a reduction reaction to grow Ag nanoparticles on the surface of UIO–66, resulting in the UIO–66@AgNPs SERS substrate (Figure 11). The Ag nanoparticles showed homogeneous distribution on the UIO–66 surface, while DEHP molecules were absorbed onto the active site of the SERS substrate through the adsorption capacity of UIO–66, thereby amplifying the Raman detection signal. Moreover, serving as a SERS substrate, UIO–66@AgNPs exhibits outstanding reliability and endurance, enabling the direct measurement of DEHP concentration in authentic plastic materials.

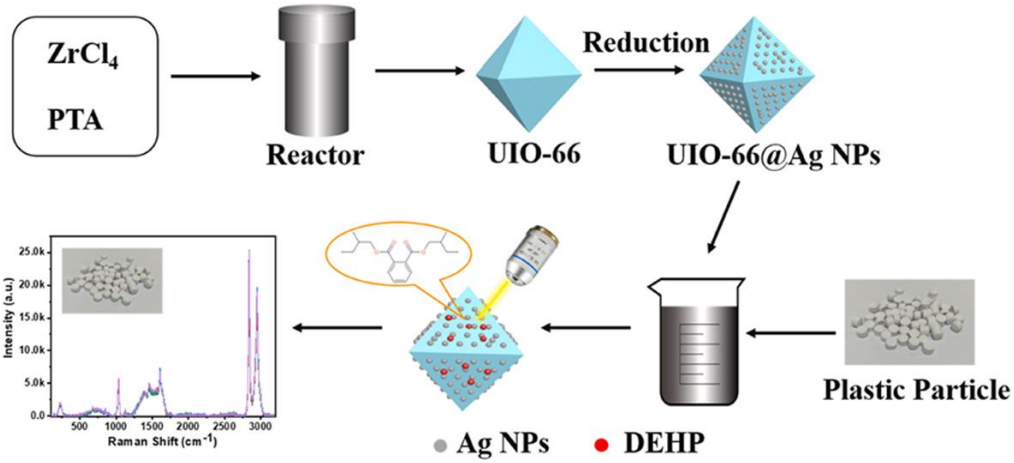

Figure 11. Fabrication of UIO–66@Ag NPs substrates and SERS analysis of DEHP in real plastic samples [53].

Current assembly methods for colloidal nanoparticles often require strong coordinating ligands on the surface of noble metals, which greatly obstruct the accessibility of analytes to the plasmonic hotspots, resulting in a substantial decrease in SERS signal strength. To prevent the aggregation of colloidal noble metal nanoparticles, Lou et al. [54] used Zr–MOFs as protective shells. The SERS substrate was first prepared by seed–mediated growth of cetyltrimethylammonium bromide (CTAB)–capped Au NRs, followed by a two–step ligand exchange process using methoxy polyethylene glycol–thiol (mPEG–SH) to replace the CTAB capping agent, hindering the agglomeration of Au NRs during the coating of MOFs onto their surfaces. Subsequently, the mPEG shell interacted with the precursor,

promoting the nucleation of Zr–MOFs on the surface of Au NRs, ultimately forming an ordered stack of Au NRs@Zr–MOFs array substrate (Figure 12a). The combination of Au NRs with a Zr–MOF composite resulted in a remarkable increase in SERS intensity during the detection of 4′–mercaptobenzonitrile molecules. The increased intensity was ascribed to the clustering of target molecules in the region between adjacent AuNRs, where the electromagnetic field experienced significant amplification. The MOF shell on the Au NRs played a crucial role in chemically and physically absorbing the target molecules, leading to their enrichment at the plasmonic gap.

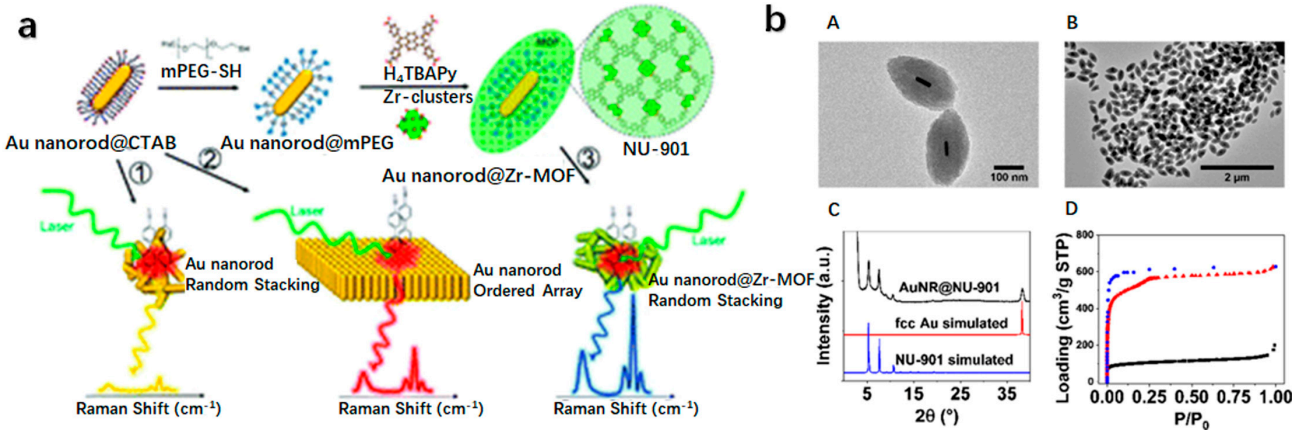

Figure 12. (**a**) Schematic representation of SERS sensing based on Au NRs@Zr–MOFs [54]. (**b**) (**b-A**), (**b-B**) TEM images, (**b-C**) XRD pattern, and (**b-D**) N_2 adsorption/desorption isotherm of AuNR@NU–901 [55].

Currently, the encapsulation of nanoparticles in MOFs is challenging to control. Jimenez et al. [55] fabricated a AuNR@NU–901 core–shell structure with uniform morphology and high yield at room temperature. The approach encompassed the functionalization of the Au NRs with polyethylene glycol surface ligands to preserve colloidal stability and facilitate MOF growth in the precursor solution. With this approach, they achieved over 99% yield of core–shell structures and could adjust the size of MOF particles based on the concentration of Au NRs in solution. The SERS substrate–based Au NR@MOFs exhibited the ability to block large molecules from entering the pores which resulted in the selective absorption of small molecules enabling highly selective SERS sensing on the substrate (Figure 12b).

3.4. Fe–MOFs/NMNPs

Fe–MOFs consist of an Fe metal center and organic ligands such as benzene dicarboxylic acid. The metal center ions in Fe–MOFs are prone to undergo Fenton–like reactions, making them suitable for photocatalysis, enzyme mimicry and other purposes. To investigate the correlation between the activity of Au NRs and Fe–MOFs as enzyme mimics under light irradiation, Meng et al. [56] successfully synthesized Au–NRs/Fe–MOF hybrids. By integrating SERS amplification with catalytic activity, they successfully monitored the identification and breakdown of the organic dye methylene blue (MB) through in situ SERS (Figure 13a). To investigate the photocatalytic mechanism of the Au–NRs/Fe–MOF composite material, the researchers first calculated the Arrhenius plot of Au–NRs/Fe–MOF (Figure 13a(B)), which indicated that the hot electrons from LSPR excitation of Au NRs lower the energy and alter the reaction pathway. Subsequently, electrochemical impedance spectroscopy (EIS) characterizations of Au–NRs/Fe–MOF with or without 660 nm laser irradiation were performed to further elucidate the charge transfer process (Figure 13a(C)). Chronoamperometric curves were used to study the photo–generated charge carriers of Au–NRs/Fe–MOF when the lamp was turned on and off (Figure 13a(D)). The results showed that under laser irradiation at the LSPR wavelength range centered on Au NRs, increased

photoinduced electrons were conveyed from the Au–NRs surface to Fe–MOF, resulting in the transformation of Fe (III) on the Fe–MOF surface into Fe (II). Fe (II) catalyzed H_2O_2 to produce ·OH radicals, which then removed MB through enhanced Fenton–like reactions. Furthermore, the Fe–MOF exhibited semiconductor properties under LSPR excitation, accepting electrons from Au NRs and suppressing the recombination of hot electrons and holes on Au NRs. Therefore, the hybridization of Au–NRs/Fe–MOFs could trigger Raman signals through the synergistic effects of CT and EM mechanisms, greatly enhancing SERS performance. The limit of detection for MB concentration could be achieved as low as 9.3×10^{-12} M.

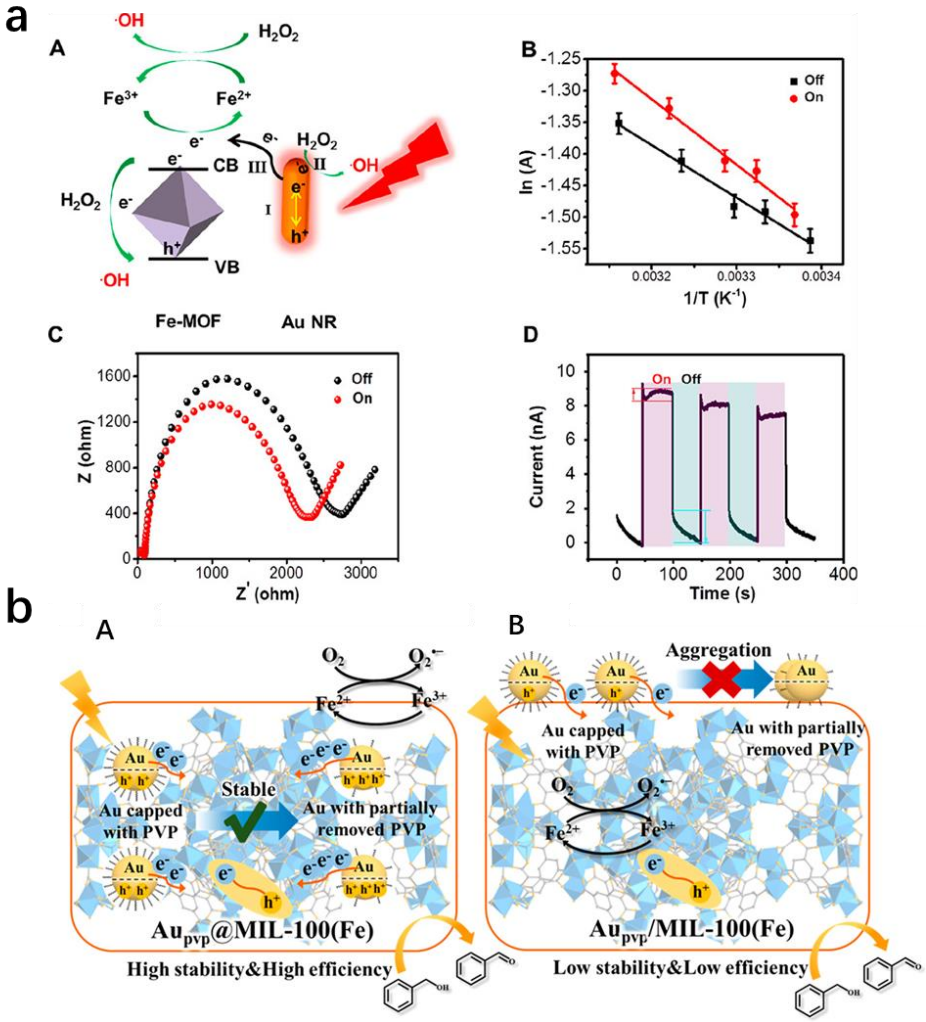

Figure 13. (**a**) (**a-A**) Diagrammatic representation of the photo–enhanced peroxidase–like activity of Au NRs/Fe–MOF under 660 nm illumination, (**a-B**) Arrhenius graph for Au NRs/Fe–MOFs under 660 nm light and in the absence of light, (**a-C**) Nyquist diagrams for Au NRs/Fe–MOFs with the light on and off, recorded at the open–circuit potential in $K_3Fe(CN)_6/K_4Fe(CN)_6$ solution, (**a-D**) chronoamperometric curves for Au NRs/Fe–MOF [56]. (**b**) Proposed mechanism for the superior photocatalytic activity over (**b-A**) Au_{pvp}@MIL–100 (Fe) and (**b-B**) Au_{rpvp}@MIL–100 (Fe) [57].

In various core–shell composite materials of NMNPs and MOFs developed throughout history, appropriate capping agents are generally added to prevent the aggregation of NMNPs. In spite of this, the stabilizing agents present around plasmonic Au nanoparticles not only hinder the active sites of plasmonic Au nanoparticles but also result in suboptimal electron transfer between MOFs and plasmonic Au nanoparticles. Therefore, in order to remove the stabilizer (PVP) from the surface of Au NPs in photocatalytic nanocomposites, Li et al. [57] employed a strategy known as "rotating bottle–around–ship" to prepare a

core–shell structured Au_{pvp}@MIL–100 (Fe) nanocomposite. Afterwards, the composite was treated with a Meerwein's salt solution to eliminate the capping agent PVP from Au_{pvp}@MIL–100 (Fe), resulting in the creation of Au_{rpvp}@MIL–100 (Fe) with a core–shell configuration (Figure 13b). The research discovered that Au_{pvp}@MIL–100 (Fe) demonstrated exceptional photocatalytic efficiency for the oxidation of benzyl alcohol under visible light, as the plasmon–induced energetic electrons migrated from the plasmonic Au NPs to MIL–100 (Fe), leading to the generation of more catalytically active $O_2^{\bullet-}$ radicals. Upon the elimination of the capping agent PVP, the charge transfer between plasmonic Au NPs and MIL–100 (Fe) was enhanced, thereby greatly enhancing the photocatalytic performance of Au_{rpvp}@MIL–100 (Fe).

3.5. Cr–MOFs/NMNPs

Cr–MOFs have a Cr metal center with tunable organic ligands. They possess a large pore size, high surface area and remarkable stability, making them excellent for adsorbing gases and other substances. To accomplish convenient and speedy optical detection of VOCs, Li et al. [58] developed a SERS platform referred to as Au NPs@MIL–101 (Cr); by incorporating Au NPs into MIL–101 (Cr), the aggregation of Au NPs is prevented, enabling the capture and identification of various gaseous VOCs (Figure 14). The presence of AuNPs inside MIL–101 (Cr) increased the microporous surface area of Au NPs@MIL–101 (Cr), allowing it to absorb a greater amount of toluene molecules, thus achieving higher detection sensitivity. Additionally, the incorporation of a significant quantity of AuNPs into MIL–101 (Cr) greatly enhanced the SERS signal. This was because the LSPR of Au NPs in Au NPs@MIL–101 (Cr) enabled a rapid and effective differentiation of different VOCs through SERS. Therefore, AuNPs@MIL–101 (Cr) could be used for multi–sensing of VOCs, even for some low Raman cross–section gaseous odors.

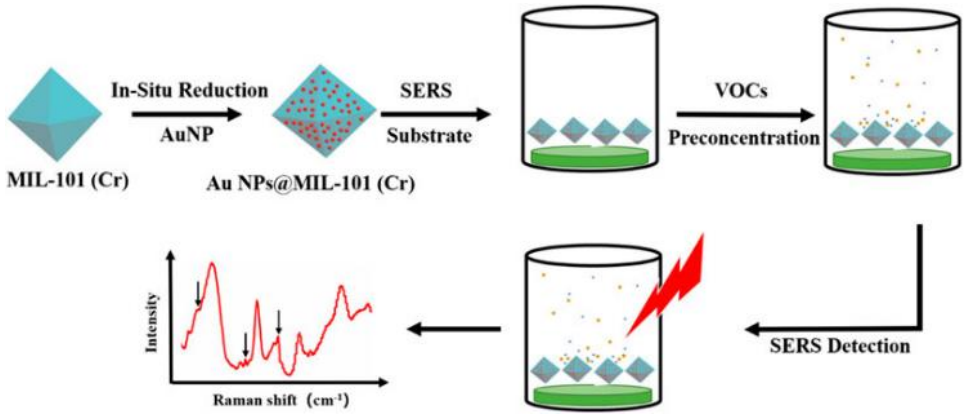

Figure 14. Schematic illustration for SERS detection of VOCs using AuNPs@MIL–101 (Cr) [58].

3.6. Cu–MOFs/NMNPs

Cu–MOFs are a class of MOFs with the transition metal Cu as the active center and various organic functional groups as ligands. Common forms of Cu–MOFs include nanosheets, octahedra and nanowires, on which researchers can load NMNPs according to their specific needs. In order to achieve non–invasive real–time blood glucose detection, Yang et al. [59] designed a SERS substrate based on multilayer nanozymes. They synthesized S–hybridized nanosheets with multiple functionalities by in situ modification of AuNPs (facilitating a uniform distribution of Au NPs on nanosheets, preventing their aggregation) onto a two–dimensional (2D) metalloporphyrin MOF (Cu–tetra(4–carboxyphenyl) porphyrin chloride (Fe (III)). This composite material was named AuNPs/Cu TCPP(Fe). The research results demonstrated that the nanosheets of AuNPs/Cu–TCPP(Fe) could exhibit a tandem enzyme activity similar to (glucose oxidase) GOx and peroxidase–like activity. When exposed to oxygen, the nanosheets composed of AuNPs/Cu TCPP(Fe) demonstrate a similar activity to GOx, facilitating the conversion of glucose into gluconic acid and H_2O_2. Addition-

ally, due to its peroxidase–like activity, it catalyzes H_2O_2, converting non–Raman–active Brilliant Green into Raman–active Brilliant Green, thereby enabling the SERS response. By exploiting this phenomenon, the precise measurement of glucose concentration was effectively achieved by tracking the SERS signal strength of the Raman–active compound Brilliant Green (Figure 15).

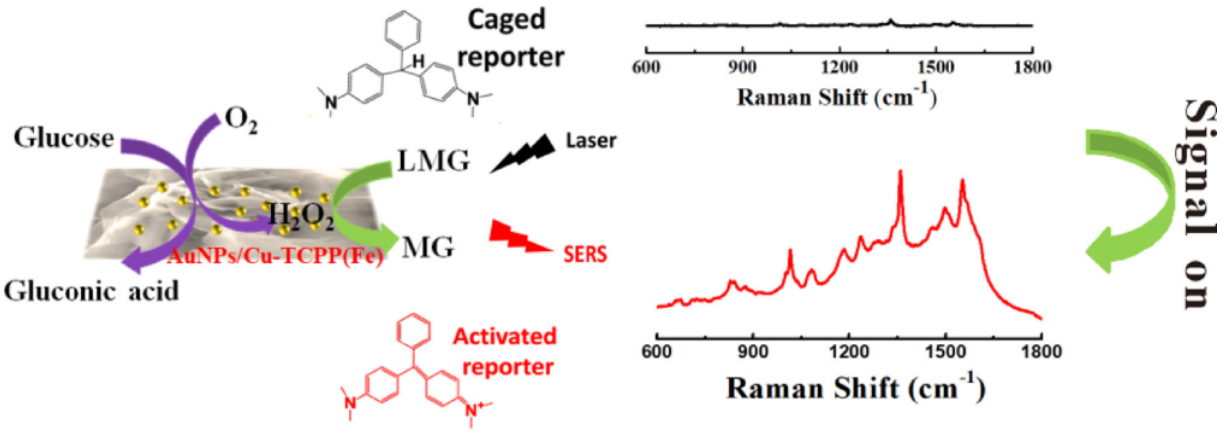

Figure 15. Diagrammatic representation of the enzyme–independent cascade reaction approach for SERS quantification of glucose [59].

4. Multicomponent SERS Substrate: MOFs/NMNPs/Others

Despite the various investigations demonstrating the successful integration of MOFs with NMNPs in the fabrication of SERS substrates, effectively merging the remarkable adsorption and enrichment capabilities of MOFs with the LSPR characteristics of NMNPs, thus significantly improving the sensitivity of SERS detection, key issues in the practical application of SERS substrates still exist as their manufacturing efficiency, uniformity, stability and multifunctionality need to be improved. To overcome the challenges posed by complex sensitive environments in practical applications, many researchers have combined MOFs, NMNPs and other materials (particularly oxides and flexible substances) to prepare composite SERS substrates that are better suited for practical use.

4.1. MOFs/NMNPs/Oxide Substances

To enhance the uniformity of the SERS substrate, Hu et al. [60] used a material of Fe_3O_4@UiO–66–NH_2@Au as the building blocks. By using Fe_3O_4 as the core, they directly grew amino–functionalized UiO–66 onto the Fe_3O_4 core, forming a uniform magnetic MOF structure (Fe_3O_4@UiO–66–NH_2) through a hydrothermal reaction. Subsequently, a new SERS substrate was acquired through in situ reduction in gold nanoparticles on the magnetic MOF surface (Figure 16a). This magnetic substrate was then used for exceedingly sensitive SERS detection, which offered numerous benefits. Firstly, UiO–66–NH_2 possesses an expansive specific surface area, enabling the integration of a larger quantity of Au NRs, leading to abundant "hot spots" and preventing Au NPs from aggregation. Secondly, the porous structure of UiO–66–NH_2, coupled with the π–π stacking of organic ligands, facilitates the absorption and concentration of aromatic samples, bringing the target molecules closer to the "hot spots". Lastly, the utilization of magnetic separation enables the sample–loaded matrix to be separated from the mixture and deposited onto the magnetic substrate, thereby reducing the occurrence of the coffee ring effect and enhancing the uniformity of the SERS substrate.

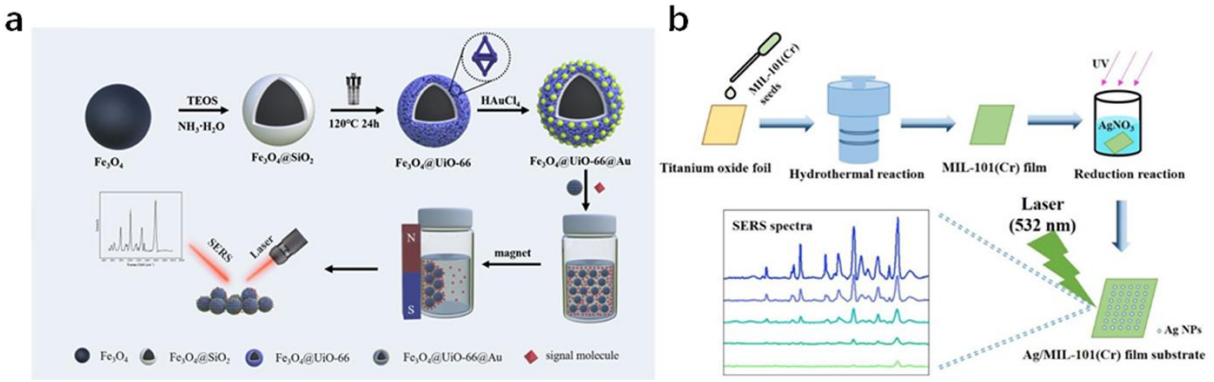

Figure 16. (**a**) Diagrammatic representation of the synthesis procedure for Fe_3O_4@UiO–66–NH_2@Au and its implementation for thiabendazole sensing using SERS [60]. (**b**) The synthesis process of SERS substrate made from Ag@MIL–101 (Cr) [61].

In order to facilitate the monitoring of complex environments in fluids, Pei et al. [61] developed a SERS substrate by combining MOF thin films with NMNPs. They fabricated a compact MIL–101 (Cr) thin film (Figure 16b) via the secondary deposition technique on textured titanium oxide substrates. Subsequently, Ag NPs were attached to the film through a UV irradiation method, resulting in a thin film of Ag@MIL–101 (Cr). Through the manipulation of UV irradiation time and the quantity of silver nitrate, a highly efficient SERS substrate film was achieved, allowing for the detection of the antibiotic furantoin.

Recently, a novel hybrid plasmonic material has gained attention in the field of SERS, consisting of both dielectric structures and metal nanostructures. This innovative approach offers advantages over traditional metal nanostructures as the presence of dielectric microstructures enables stronger concentration of optical power onto the metal nanostructures. This results in a more pronounced amplification of the electromagnetic field. To create more sensitive SERS substrates utilizing plasmonic structures, Huang et al. [62] combined the photonic microstructure of SiO_2 microspheres with Ag NP@ZIF–8 thin films to obtain a hybrid plasmonic substrate. The Ag NP@ZIF–8 thin film was a 2D plasmonic film formed through an organic–water interface self–assembly process, and SiO_2 was added to form the hybrid plasmonic substrate (Figure 17). The hybrid plasmonic structure discussed here possesses the ability to adsorb gases, making it suitable as a SERS substrate for the detection of 4–mercaptophenol gas. Empirical evidence suggested that the SERS efficiency of this substrate was impacted by the ZIF shell thickness and the dimensions of SiO_2 microspheres.

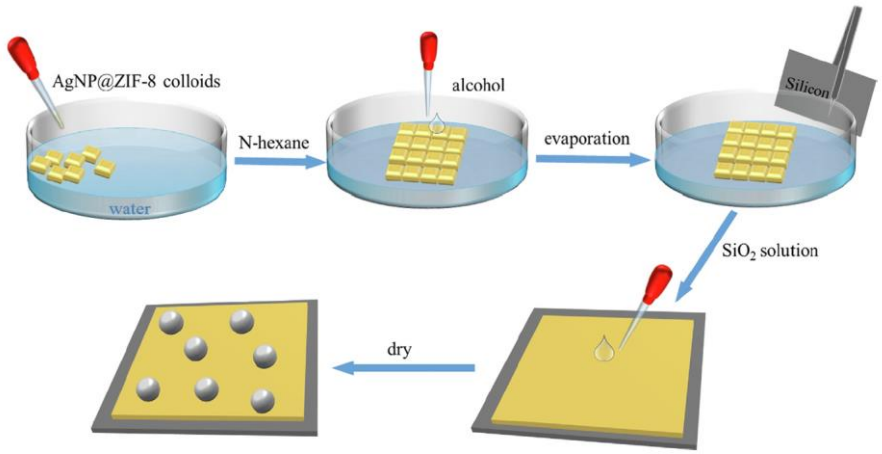

Figure 17. The fabrication process of optoplasmonic MOF film [62].

4.2. MOFs/NMNPs/Flexible Substances

Anchoring metal nanostructures onto flexible carriers such as fibers or polymer films through techniques such as dipping and electrostatic spraying may offer advantages of low cost, disposable use and ease of manufacturing to the SERS substrates. Jiang et al. [63] utilized plasma technology to reduce Au NPs on cellulose paper and then synthesized Au NPs@ZIF–8 cellulose film by coating Au NPs with ZIF–8 (Figure 18a). ZIF–8 could be loaded onto cellulose paper mainly because zinc ions could form coordination bonds with carboxyl groups on the paper. The adaptable SERS substrate, modified with 4–MBA, was employed for quantitative SERS analysis of cadaverine and putrescine. In this context, the 4–MBA molecules served as both Raman reporter entities and selective binders for the volatile amine molecules.

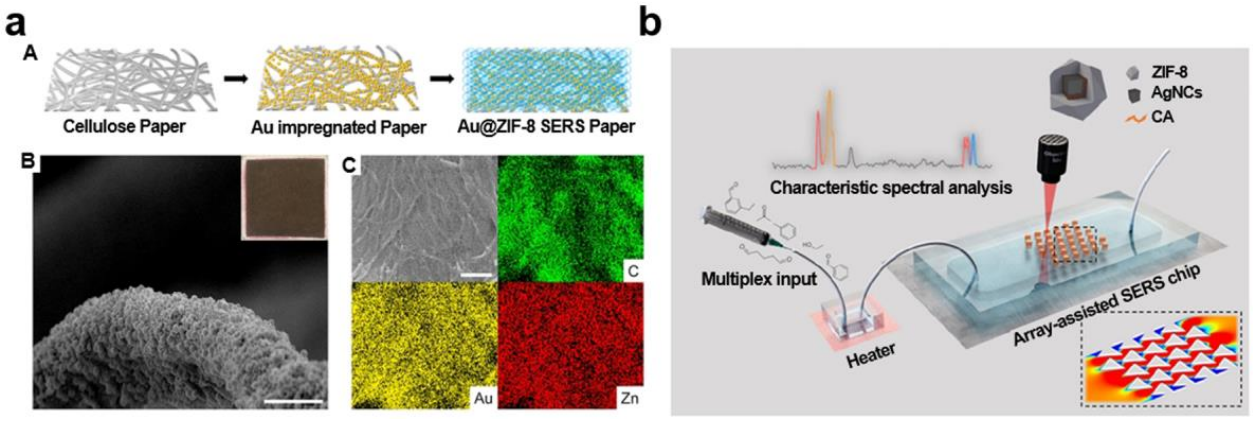

Figure 18. (**a**) (**a-A**) Schematic representation of the fabrication process of Au@ZIF–8 substrate, (**a-B**) SEM side view image of Au@ZIF–8, scale bar: 5 μm, inset is a photograph of the SERS substrate, and (**a-C**) EDX elemental mapping images of Au@ZIF–8, scale bar: 5 μm [63]. (**b**) Diagrammatic representation of array SERS chip [64].

Flexible SERS substrates demonstrate excellent capability to tightly contact with any surface, providing significant advantages in rapid sampling and detection. In order to enhance the adsorption efficiency of gas detection and improve the signal–to–noise ratio, Cui et al. [64] designed a microfluidic SERS chip array with prism holes (Figure 18b). They first prepared Au@AgNCs@ZIF–8 composite materials and then modified them with cysteamine (CA) for specific recognition and capture of aldehydes as SERS probes. Subsequently, the modified composite materials were coated onto the surface of the prism holes, where they would remain at the top due to electrostatic interactions. Experimental results show that this SERS probe structure can further enhance the gas adsorption capacity of ZIF–8, and the SERS background of CA is lower. Additionally, based on the inherent SERS signal of CA, simultaneous detection of multiple gases can be easily achieved.

5. Application of Gas Sensing

The monitoring of dangerous and harmful gases in the surrounding atmosphere is vital for managing air pollution, averting environmental catastrophes, evaluating situations and notifying the public about potential acts of terrorism [65]. In the case of NMNPs, typically, favorable SERS signals from molecules can only be obtained when they are in close proximity to the nanostructure surface through chemical or physical interactions (distance < 5 nm). Gas molecules, compared to liquid or solid molecules, diffuse more rapidly and are harder to capture. However, MOFs, as porous materials, can reduce the diffusion rate of gases. Therefore, designing novel sensing systems based on the combination of NMNPs with MOFs shows great potential in gas molecule detection. Currently, using NMNPs and MOF composites as SERS substrates enables real–time detection of VOCs, psychoactive agents, greenhouse gases and other pollutant mixtures [66]. Currently, researchers are primarily using the pore size of MOFs to selectively screen mixed

gases, excluding large molecules while allowing small molecules to enter the MOF for SERS analysis. On the other hand, by modifying the SERS substrate with probe molecules (such as 4–aminothiophenol), specific reactions (e.g., amidation reactions) can be utilized for targeted recognition of similar gas molecules. Further development of more specific reactions remains to be explored. Additionally, researchers can introduce other specific species to prepare MOF–based SERS substrates, such as magnetic or fluorescent materials, to enhance substrate selectivity. This simplifies the SERS detection process and improves sensing performance.

5.1. Detection of VOCs

Some molecules, especially VOC gases, can cause severe damage to the human nervous system and hematopoietic function. They are difficult to adsorb on substrates and do not interact with SERS substrates, thereby limiting the acquisition of clean molecular Raman signals. Li et al. [67] synthesized SERS substrates with a Au NPs@ZIF–8 core–shell structure for the SERS detection of weakly adsorbed molecules (Figure 19). By adjusting the precursor ions, the shell thickness of individual Au NPs@ZIF–8 could be precisely controlled within the range of 3 to 8 nm, thus adjusting the distance and electromagnetic field interactions among the metallic nanoparticles. By harnessing the remarkable gas adsorption properties of the ZIF–8 shell in combination with the pronounced SPR effect of Au NPs, the Au NPs@ZIF–8 composite, with a precisely tailored shell thickness of 3 nm, emerged as an appealing core–shell structure. This composite proved to be exceptionally suitable for monitoring variations in toluene through time–dependent SERS spectra, as well as enabling the specific identification of diverse VOC gases such as toluene, ethylbenzene and chlorobenzene.

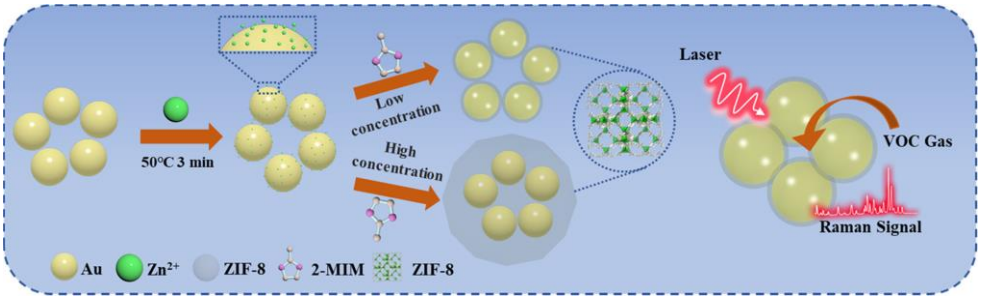

Figure 19. Illustrated synthesis of Au@ZIF–8 and its application in VOC gas detection [67].

The accurate, responsive and specific on–site detection of volatile aldehydes, which act as indicators for lung cancer, holds immense importance in the early–stage diagnosis and therapeutic direction of cancer. To overcome challenges faced during on–site screening, such as time consumption, the need for specialized personnel and the complexity of the matrix, Deng et al. [68] devised a novel platform called the vapor generation paper–based thin film microextraction (VG–PTFM). This platform incorporated fluorescence (FL) and SERS sensing, utilizing a core–shell structure of gold nanorod quantum dots (GNRs–QDs) @NU–901, specifically designed for detecting volatile benzaldehyde (BA) (Figure 20). This platform enables the precise quantification of BA through sensitive on–site fluorescence detection and accurate SERS analysis. The amino–functionalized GNRs and carboxyl–terminated quantum dots can directly assemble through electrostatic interactions, resulting in nearly complete quenching of the quantum dot emission. The incorporation of BA molecules, facilitated by the Schiff base reaction between the amine moiety of 4–mercaptobenzenamine and the aldehyde moiety of BA, disrupts the arrangement of GNRs–QDs. This disruption leads to an enhancement in both fluorescence and Raman signals within the hybrid system, enabling the visual identification of BA. Additionally, the porous MOF shell's "cavity diffusion" effect confirms the preferential accumulation of gaseous BA molecules on the surface of GNRs, enabling rapid and accurate differentiation

of exhaled BA. This discrimination can be achieved even at ultra–low concentrations of sub–parts–per–billion levels, demonstrating exceptional specificity towards other VOCs.

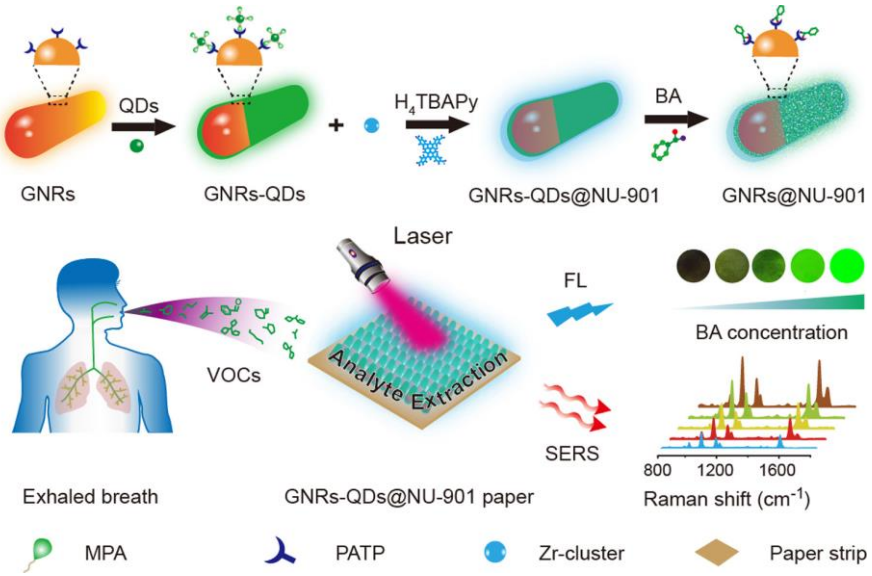

Figure 20. Dual–mode sensing of volatile biomarkers in human breath using AuNRs–QDs@NU–901 [68].

Gaseous molecules exhibit faster diffusion rates compared to liquid and solid molecules due to the increased intermolecular space. Nonetheless, this increased rate of diffusion may potentially result in insufficient interaction between the gas under analysis and the solid matrix. In order to improve the adsorption of gaseous molecules, Wang et al. [45] developed a SERS substrate called GSPs@ZIF–8. The use of a ZIF–8 layer on the self–assembled GSPs successfully decreased the gas biomarkers' flow rate and mitigated the exponential decline of the electromagnetic field surrounding the GSPs surface (Figure 21). The substrate selectively trapped gaseous aldehydes onto the GSPs substrate through a Schiff base reaction involving the Raman–active probe molecule 4–ATP. As a consequence, even in intricate mixtures of VOCs, the SERS signal of 4–ATP demonstrated discernible variations in reaction to aldehyde in VOCs, descending to levels as minute as ppb. This underscores the immense capability of this technology in the context of early lung cancer screening endeavors.

5.2. Detection of Psychoactive Agents

Biological and chemical weapons, as a form of mass destruction, continue to pose a threat to human life and safety at all times. The identification, quantification and monitoring of harmful substances in the atmosphere are vital for managing air pollutants, averting environmental catastrophes and informing the public about the possible employment of chemical weapons in acts of terrorism. For instance, Mallada et al. [69] reported a plasma adsorbent thin film platform with integrated Raman internal standards, which exhibited excellent SERS detection performance towards chemical warfare agent simulants. In the SERS film, a closely arranged core–shell structure was formed using Au@Ag nanorods enclosed within a ZIF–8 framework (Au@Ag@ZIF–8) (Figure 22). By incorporating Au@Ag nanoparticles, the Raman signals of molecules in close proximity were significantly enhanced. Simultaneously, the ZIF–8 structure played a vital role as the capturing agent for di–methyl methylphosphonate (DMMP) or 2–chloroethyl ethyl sulfide (CEES) in the gaseous state, while also functioning as the Raman reference standard. Through computational simulations, they successfully investigated the potential adsorption mechanisms of molecules within the ZIF–8 framework and the interactions between DMMP and the surface of Ag. The Au@Ag@ZIF–8 film displayed exceptional SERS performance for DMMP and CEES, with excellent response time, detection limit, reproducibility and recyclability.

Specifically, the detection limit for DMMP reached 0.2 ppbV. Furthermore, using a portable Raman instrument, the experimental detection achieved a recognition of 2.5 ppmV of DMMP in the surrounding air and 76 parts ppbV of CEES in N_2, with respective response durations of 21 and 54 s. This proof–of–concept has the potential to revolutionize the practical implementation of SERS–based handheld gas sensing for ultra–low concentrations. It can be utilized in diverse domains including national security, safeguarding critical infrastructure, chemical processes monitoring, and personalized healthcare.

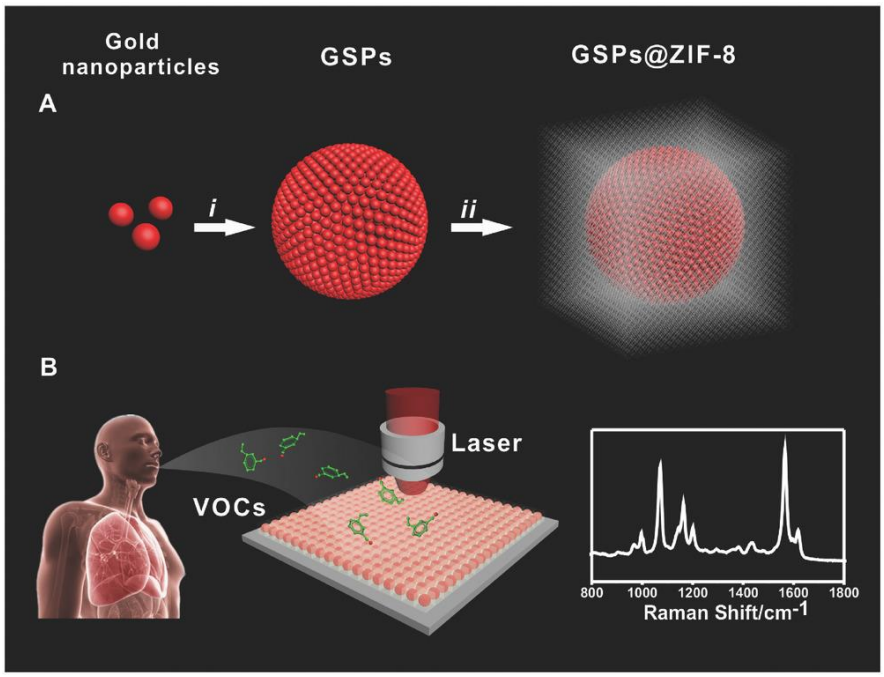

Figure 21. (**A**) Diagrammatic sketch of synthesizing GSP@ZIF-8 core–shell structure: (i) gold nanoparticles assembled into GSPs, (ii) ZIF-8 shell coated on GSP surface. (**B**) VOC detection via SERS spectroscopy [45].

5.3. Detection of Greenhouse Gases

China has long been dedicated to the combustion of fossil fuels such as coal and gasoline to supplement electricity, transportation and heating [70]. Consequently, the atmosphere becomes burdened with substantial quantities of greenhouse gases such as carbon dioxide (CO_2), nitrous oxide (N_2O), hydrofluorocarbons (HFCs), perfluorocarbons (PFCs), sulfur hexafluoride (SF_6) and methane. These greenhouse gas molecules possess the ability to trap heat by absorbing and subsequently re–emitting radiation within the thermal infrared range of the Earth's surface. This process culminates in the greenhouse effect, wherein heat is retained in the atmosphere. In order to facilitate the capture and detection of CO_2, Huang et al. [71] synthesized PVP–modified Ag nanowires using the solvent–thermal polyol method, followed by coating Au nanoparticles onto the Ag nanowires to create a hybrid dual–functional nanostructure. The Ag@Au composite nanowires were further developed by ultra–thin ZIF–8 to form Ag@Au@ZIF–8 NWs/TF composite as the SERS substrates. The presence of the ZIF–8 coating on this substrate effectively inhibits the oxidation of Ag nanowires. Due to the matching pore size of ZIF–8 (3.4 Å) with the size of CO_2 molecules (3.33 Å), the SERS substrate exhibited higher selectivity and adsorption performance for the capture and detection of CO_2 (Figure 23). Increasing the duration of enrichment to 8 min results in the characteristic peak associated with the symmetric tensile vibration of CO_2 reaching its maximum intensity. Remarkably, this maximum intensity is equivalent to the intensity achieved after 30 min of enrichment. This implies that the ZIF–8 shell requires only 8 min to adsorb a sufficient concentration of CO_2, reaching the threshold necessary for detection of the SERS signal.

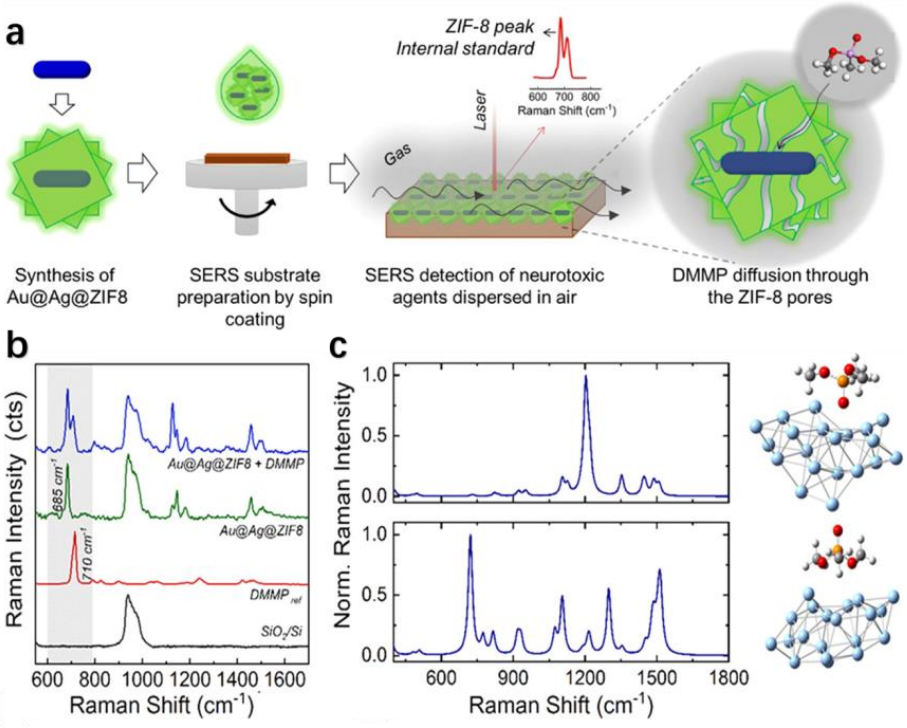

Figure 22. (**a**) Manufacturing schematic of Au@Ag@ZIF–8 SERS substrate for the detection of neurotoxic agents in the gas phase in the air. (**b**) SERS spectrum of 2.5 ppmV DMMP in nitrogen (N_2), captured on thin films made of Au@Ag@ZIF–8. References also encompass the Raman spectra of SiO_2/Si substrates and liquid–phase DMMP, along with the SERS spectrum obtained from the Au@Ag@ZIF–8 thin film. (**c**) Raman spectra for Ag_{20}–DMMP complexes calculated for different orientations [69].

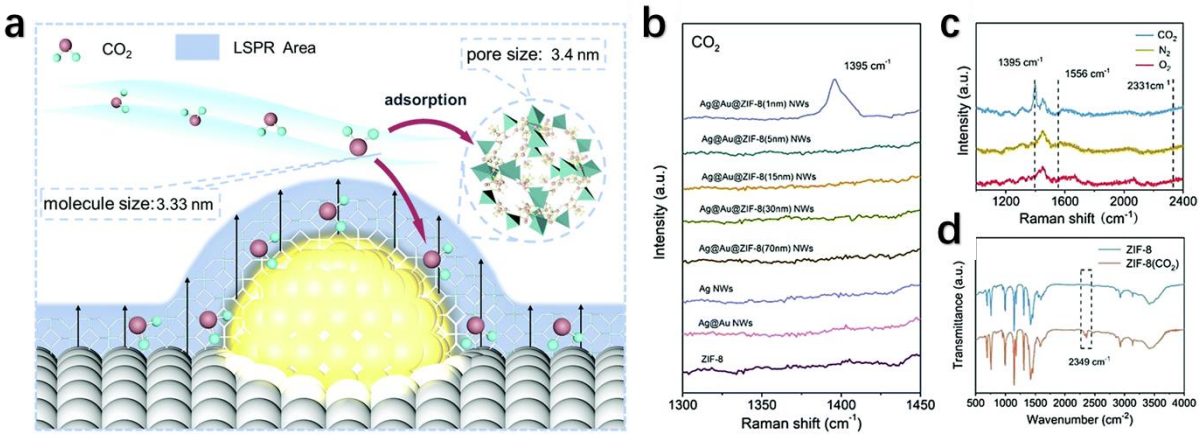

Figure 23. (**a**) Enrichment method for CO_2 gas molecules and mechanism of SERS amplification. (**b**) SERS spectra of individual Ag@Au@ZIF–8 NWs/TF coated with ZIF–8 shells of 1 nm, 5 nm, 15 nm, 30 nm and 70 nm thicknesses, as well as individual Ag NWs, Ag@Au NWs, and individual ZIF–8 spheres, in the presence of CO_2 at room temperature. (**c**) SERS spectra of individual Ag@Au@ZIF–8 core/shell nanowires with a ZIF–8 shell thickness of 1 nm, upon exposure to CO_2, N_2 and O_2. (**d**) IR spectrum of ZIF–8 before and after the adsorption of CO_2 [71].

6. Conclusions and Prospect

This article introduces the advantages and functionalities of using a single MOF material as a SERS substrate and focuses on the design and synthesis of composite materials composed of MOFs and NMNPs with different metal centers, with a particular emphasis on their applications in optical gas sensing.

In recent decades, MOFs have garnered significant attention in conventional domains owing to their remarkable characteristics and distinctive architectures. More and more MOFs with different metal centers have been discovered, and the diverse properties and characteristics of MOFs with various metal cores have been investigated. The unique structure and characteristics of MOFs have also fostered the advancement of SERS, particularly with regards to discerning detection and gas sensing. MOFs with different metal centers possess distinct advantages, and MOFs with specific metal centers can be selectively introduced based on the substances detected by the SERS substrate. Apart from harnessing the chemical characteristics and thermal stability of MOFs, the active sites of specific metal centers can be utilized to study the SERS detection mechanism and energy transfer, which favors the production of SERS substrates for gas sensing. MOFs have unique advantages in gas sensing: (i) they can achieve rapid separation/concentration of gas molecules and selectively absorb molecules based on their size, (ii) MOFs can interact with analytes through charge transfer to achieve chemical enhancement, and (iii) MOFs can be modified or designed to detect specific gas targets. These advantages provide great potential for MOFs in gas sensing performance in SERS and offer opportunities for efficient gas detection.

Although the combination of MOFs and NMNPs offers numerous opportunities for gas detection using SERS technology, there are still challenges that need to be overcome: (i) specific enrichment and identification mechanisms for trace target molecules in SERS hotspots; (ii) the stability, reproducibility, and repeatability of SERS substrates in complex interfering environments (including humidity, temperature, etc.); (iii) simultaneous detection of multiple gas pollutants using SERS substrates in practical applications; and (iv) miniaturization of SERS platforms to enable real–time gas detection. To meet the practical application requirements of SERS substrates in gas detection, it is imperative to tackle these concerns and lay the groundwork for the continued progression of SERS–based gas sensing in domains like security and defense, healthcare, environmental monitoring, agriculture and the food sector.

When developing and preparing MOF–based SERS substrates in the future, researchers need to consider the following aspects: (1) intrinsic properties of MOFs, such as pore size, stability and structure; (2) localized surface plasmon resonance effects of noble metal particles; and (3) physical and chemical properties of the target gas for detection. Overall, there are no fixed criteria for material selection. However, we can utilize advanced techniques such as lithography, vapor deposition, sputtering and microfluidics to purposefully design patterned and versatile MOF–based SERS substrates for gas analysis.

Author Contributions: Writing—original draft preparation: W.X., X.W. and H.L.; supervision: Y.Z. All authors have read and agreed to the published version of the manuscript.

Funding: This work was financially supported by The National Key Research and Development Program of China (No. 2021YFD1700300).

Institutional Review Board Statement: Not applicable.

Informed Consent Statement: Not applicable.

Data Availability Statement: Not applicable.

Conflicts of Interest: The authors declare no conflict of interest.

References

1. Ogbeide, O.; Bae, G.; Yu, W.; Morrin, E.; Song, Y.; Song, W.; Li, Y.; Su, B.; An, K.; Hasan, T. Inkjet–printed rGO/binary metal oxide sensor for predictive gas sensing in a mixed environment. *Adv. Funct. Mater.* **2022**, *32*, 211334. [CrossRef]
2. Zhang, Y.; Jiang, Y.; Yuan, Z.; Liu, B.; Zhao, Q.; Huang, Q.; Li, Z.; Zeng, W.; Duan, Z.; Tai, H. Synergistic effect of electron scattering and space charge transfer enabled unprecedented room temperature NO_2 sensing response of SnO_2. *Small* **2023**, *19*, 2303631. [CrossRef]
3. Wu, K.; Debliquy, M.; Zhang, C. Metal–oxide–semiconductor resistive gas sensors for fish freshness detection. *Compr. Rev. Food Sci. Food Saf.* **2023**, *22*, 913–945. [CrossRef]

4. Jung, G.; Kim, J.; Hong, S.; Shin, H.; Jeong, Y.; Shin, W.; Kwon, D.; Choi, E.; Lee, J. Energy efficient artificial olfactory system with integrated sensing and computing capabilities for food spoilage detection. *Adv. Sci.* **2023**, *9*, 230250. [CrossRef]
5. Xu, F.G.; Shang, W.J.; Ma, G.R.; Zhu, Y.M.; Wu, M.J. Metal organic framework wrapped gold nanourchin assembled on filter membrane for fast and sensitive SERS analysis. *Sens. Actuat. B–Chem.* **2021**, *326*, 128968. [CrossRef]
6. Tang, W.; Chen, Z.; Song, Z.; Wang, C.; Wan, C.; Jonathan Chan, C.; Chen, Z.; Ye, W.; Fan, Z. Microheater integrated nanotube array gas sensor for parts–per–trillion level gas detection and single sensor–based gas discrimination. *ACS Nano* **2022**, *16*, 10968–10978. [CrossRef]
7. Li, C.; Choi, P.; Masuda, Y. Highly sensitive and selective gas sensors based on NiO/MnO_2@NiO nanosheets to detect allyl mer–captan gas released by humans under psychological stress. *Adv. Sci.* **2022**, *9*, 22024.
8. Yu, W.; Xie, W.; Wang, L.; Lv, Q.; Jiang, Y.; Zhang, W.; Huang, C.; Wang, L.; Huang, Y. Metal–organic framework nanoparticle films for surface–enhanced Raman spectroscopy–based autograding in the odor intensity of gas mixture generated from kitchen waste. *ACS Appl. Mater. Interfaces* **2022**, *5*, 15142–15149. [CrossRef]
9. Ivo, S.; Nicholas, C.B.; Alec, T.; Paolo, F.; Mark, D.A.; Rob, A. An updated roadmap for the integration of metal–organic frameworks with electronic devices and chemical sensors. *Chem. Soc. Rev.* **2017**, *46*, 3185.
10. Xu, F.G.; Xuan, M.R.; Ben, Z.X.; Shang, W.J.; Ma, G.R. Surface enhanced Raman scattering analysis with filter–based enhancement substrates: A mini review. *Rev. Anal. Chem.* **2021**, *40*, 75–92. [CrossRef]
11. Han, H.; Cho, S.; Han, S.; Jang, J.; Lee, G.; Cho, E.; Kim, S.; Kim, I.; Jang, M.; Tuller, H.; et al. Synergistic integration of chemo–resistive and SERS sensing for label–free multiplex gas detection. *Adv. Mater.* **2021**, *33*, 2105199. [CrossRef] [PubMed]
12. Wang, X.; Huang, S.; Hu, S.; Yan, S.; Ren, B. Fundamental understanding and applications of plasmon–enhanced Raman spectroscopy. *Nat. Rev. Phys.* **2020**, *2*, 253–271. [CrossRef]
13. Guselnikova, O.; Lim, H.; Kim, H.; Kim, H.; Gorbunova, A.; Eguchi, M.; Postnikov, P.; Nakanishi, T.; Asahi, T.; Na, G.; et al. New trends in nanoarchitectured SERS substrates: Nanospaces, 2D materials, andorganic heterostructures. *Small* **2022**, *18*, 2107182. [CrossRef]
14. Ding, S.; You, E.; Tian, Z.; Moskovits, M. Electromagnetic theories of surface–enhanced Raman spectroscopy. *Chem. Soc. Rev.* **2017**, *46*, 4042–4076. [CrossRef] [PubMed]
15. Li, C.; Xu, S.; Yu, J.; Li, Z.; Li, W.; Wang, J.; Liu, A.; Man, B.; Yang, S.; Zhang, C. Local hot charge density regulation: Vibration–free pyroelectric nanogenerator for effectively enhancing catalysis and in–situ surface enhanced Raman scattering monitoring. *Nano Energy* **2021**, *81*, 105585. [CrossRef]
16. Ye, C.; He, C.; Zhu, Z.; Shi, X.; Zhang, M.; Bao, Z.; Huang, Y.; Jiang, C.; Lie, J.; Wu, Y. A portable SERS sensing platform for the multiplex identification and quantification of pesticide residues on plant leaves. *J. Mater. Chem. C* **2022**, *10*, 12966–12974. [CrossRef]
17. Lee, H.; Lee, Y.; LinKoh, C.; Phan–Quang, G.; Han, X.; Lay, C.; Fan Sim, H.; Kao, Y.; An, Q.; Ling, X. Designing surface–enhanced Raman scattering (SERS) platforms beyond hotspot engineering: Emerging opportunities in analyte manipulations and hybrid materials. *Chem. Soc. Rev.* **2019**, *48*, 731–756. [CrossRef]
18. Cai, J.; Wang, Z.; Jia, S.; Feng, Z.; Ren, Y.; Lin, L.; Chen, G.; Eng, Z. $Si/TiO_2/Ag$ multistorey structures with interfacial charge transfer for a recyclable surface–enhanced Raman scattering substrate. *ACS Appl. Mater. Interfaces* **2022**, *14*, 13703–13712. [CrossRef]
19. Wang, X.; Guo, L. SERS Activity of Semiconductors: Crystalline and Amorphous Nanomaterials. *Angew. Chem. Int. Ed.* **2019**, *59*, 4231–4239. [CrossRef]
20. He, M.; Yu, Y.; Wang, J. Biomolecule–tailored assembly and morphology of gold nanoparticles for LSPR applications. *Nano Today* **2020**, *35*, 101005. [CrossRef]
21. Liu, H.; Zeng, J.; Song, L.; Zhang, L.; Chen, Z.; Li, J.; Xiao, Z.; Su, F.; Huang, Y. Etched–spiky Au@Ag plasmonic–superstructure monolayer films for triple amplification of surface–enhanced Raman scattering signals. *Nanoscale Horiz.* **2022**, *7*, 554–561. [CrossRef] [PubMed]
22. Liu, X.; Ye, Z.; Xiang, Q.; Xu, Z.; Yue, W.; Li, C.; Xu, Y.; Wang, L.; Cao, X.; Zhang, J. Boosting electromagnetic enhancement for detection of non–adsorbing analytes on semiconductor SERS substrates. *Chem* **2023**, *9*, 1464–1476. [CrossRef]
23. Hartland, G.V.; Besteiro, L.V.; Johns, P.; Govorov, A.O. What's so Hot about Electrons in Metal Nanoparticles? *ACS Energy Lett.* **2017**, *2*, 1641–1653. [CrossRef]
24. Sunil, J.; Narayana, C.; Kumari, G.; Jayaramulu, K. Raman spectroscopy, an ideal tool for studying the physical properties and applications of metal–organic frameworks (MOFs). *Chem. Soc. Rev.* **2023**, *52*, 3397–3437. [CrossRef]
25. Tan, L.; Wei, M.; Shang, L.; Yang, Y. Cucurbiturils–mediated noble metal nanoparticles for applications in sensing, SERS, theranostics, and catalysis. *Adv. Funct. Mater.* **2020**, *31*, 2007277. [CrossRef]
26. Lai, H.; Li, G.; Xu, F.; Zhang, Z. Metal–organic frameworks: Opportunities and challenges for surface–enhanced Raman scattering—A review. *J. Mater. Chem. C* **2020**, *8*, 2952–2963. [CrossRef]
27. Zhang, Y.; Xue, C.; Xu, Y.; Cui, S.; Ganeev, A.; Kistenev, Y.; Gubal, A.; Chuchina, V.; Jin, H.; Cui, D. Metal–organic frameworks–based surface–enhanced Raman spectroscopy technique for ultra–sensitive biomedical trace detection. *Nano Res.* **2023**, *16*, 2968–2979. [CrossRef]
28. Furukawa, H.; Cordova, K.; O'Keeffe, M.; Yaghi, O. The chemistry and applications of metal–organic frameworks. *Science* **2013**, *341*, 1230444. [CrossRef]

29. Yuan, H.; Li, N.; Fan, W.; Cai, H.; Zhao, D. Metal–organic framework based gas sensors. *Adv. Sci.* **2021**, *9*, 2104374. [CrossRef]
30. Lin Koh, C.S.; Lee, H.K.; Han, X.; Fan Sima, H.Y.; Ling, X.Y. Plasmonic nose: Integrating the MOF–enabled molecular preconcentration effect with a plasmonic array for recognition of molecular–level volatile organic compounds. *Chem. Commun.* **2018**, *54*, 2546–2549.
31. Peng, Y.; Wei, X.; Wang, Y.; Li, W.; Zhang, S.; Jin, J. Metal–organic framework composite photothermal membrane for removal of high–concentration volatile organic compounds from water via molecular sieving. *ACS Nano* **2022**, *16*, 8329–8337. [CrossRef]
32. Chang, K.; Zhao, Y.; Wang, M.; Xu, Z.; Zhu, L.; Xu, L.; Wang, Q. Advances in metal–organic framework–plasmonic metal composites based SERS platforms: Engineering strategies in chemical sensing, practical applications and future perspectives in food safety. *Chem. Eng. J.* **2023**, *459*, 141539. [CrossRef]
33. Wang, P.; Sun, Y.; Li, X.; Wang, L.; Xu, Y.; Li, G. Recent advances in metal organic frameworks based surface enhanced Raman scattering substrates: Synthesis and application. *Molecules* **2021**, *26*, 209. [CrossRef]
34. Brunner, E.; Rauche, M. Solid–state NMR spectroscopy: An advancing tool to analyse the structure and properties of metal–organic frameworks. *Chem. Sci.* **2020**, *11*, 4297–4304. [CrossRef]
35. Huang, C.; Li, A.; Chen, X.; Wang, T. Understanding the role of metal–organic frameworks in surface–enhanced Raman scattering application. *Small* **2020**, *16*, 2004802. [CrossRef]
36. Van Wyk, A.; Smith, T.; Park, J.; Deria, P. Charge–transfer within Zr–based metal–organic framework: The role of polar node. *J. Am. Chem. Soc.* **2018**, *140*, 2756–2760. [CrossRef]
37. Huang, C.; Dong, J.; Sun, W.; Xue, Z.; Ma, J.; Zheng, L.; Liu, C.; Li, X.; Zhou, K.; Qiao, X.; et al. Coordination mode engineering in stacked–nanosheet metal–organic frameworks to enhance catalytic reactivity and structural robustness. *Nat. Commun.* **2019**, *10*, 2779. [CrossRef]
38. Zong, C.; Xu, M.; Xu, L.; Wei, T.; Ma, X.; Zheng, X.; Hu, R.; Ren, B. Surface–enhanced Raman spectroscopy for bioanalysis: Reliability and challenges. *Chem. Rev.* **2018**, *118*, 4946–4980. [CrossRef]
39. Sun, H.; Song, G.; Gong, W.; Lu, W.; Cong, S.; Zhao, Z. Stabilizing photo–induced vacancy defects in MOFs matrix for high–performance SERS detection. *Nano Res.* **2022**, *15*, 5347–5354. [CrossRef]
40. Sun, H.; Cong, S.; Zheng, Z.; Wang, Z.; Chen, Z.; Zhao, Z. Metal–organic frameworks as surface enhanced Raman scattering substrates with high tailorability. *J. Am. Chem. Soc.* **2019**, *141*, 870–878. [CrossRef]
41. Fu, J.; Zhong, Z.; Xie, D.; Guo, Y.; Kong, D.; Zhao, Z.; Zhao, Z.; Li, M. SERS–active MIL–100(Fe) sensory array for ultrasensitive and multiplex detection of VOCs. *Angew. Chem. Int. Ed.* **2020**, *59*, 20489–20498. [CrossRef] [PubMed]
42. Chen, Z.; Su, L.; Ma, X.; Duan, Z.; Xiong, Y. A mixed valence state Mo–based metal–organic framework from photoactivation as a surface–enhanced Raman scattering substrate. *New J. Chem.* **2021**, *45*, 5121–5126. [CrossRef]
43. Phan–Quang, G.C.; Yang, N.; Lee, H.K.; Fan Sim, H.Y.; Lin Koh, C.S.; Kao, Y.-C.; Wong, Z.C.; Ming Tan, E.K.; Miao, Y.-E.; Fan, W.; et al. Tracking airborne molecules from afar: Three–dimensional metal–organic framework–surface–enhanced Raman scattering platform for stand–off and real–time atmospheric monitoring. *ACS Nano* **2019**, *13*, 12090–12099. [CrossRef] [PubMed]
44. Ben, Z.X.; Ma, G.R.; Xu, F.G. UIO–66/Ag/TiO_2 Nanocomposites as Highly Active SERS Substrates for Quantitative Detection of Hexavalent Chromium. *Chemosensors* **2023**, *11*, 315. [CrossRef]
45. Qiao, X.; Su, B.; Liu, C.; Song, Q.; Luo, D.; Mo, G.; Wang, T. Selective surface enhanced Raman scattering for quantitative detection of lung cancer biomarkers in superparticle@MOFs structure. *Adv. Mater.* **2018**, *30*, 1702275. [CrossRef]
46. Li, A.; Qiao, X.; Liu, K.; Bai, W.; Wang, T. Hollow metal organic framework improves the sensitivity and anti–interference of the detection of exhaled volatile organic compounds. *Adv. Funct. Mater.* **2022**, *32*, 30–2202805. [CrossRef]
47. Xie, X.; Zhang, Y.; Zhang, L.; Zheng, J.; Huang, Y.; Fa, H. Plasmon–driven interfacial catalytic reactions in plasmonic MOFs nanoparticles. *Anal. Chem.* **2021**, *93*, 13219–13225. [CrossRef]
48. Ding, Q.; Wang, J.; Chen, X.; Liu, H.; Li, Q.; Wang, Y.; Yang, S. Quantitative and sensitive SERS platform with analyte enrichment and filtration function. *Nano Lett.* **2020**, *20*, 7304–7312. [CrossRef]
49. Yang, X.; Liu, Y.; Lam, S.; Wang, J.; Wen, S.; Yam, C.; Shao, L.; Wang, J. Site–selective deposition of metal–organic frameworks on gold nanobipyramids for surface–enhanced Raman scattering. *Nano Lett.* **2021**, *21*, 8205–8212. [CrossRef]
50. Zhang, Y.; Lu, C.; Lin, Q.; Yu, J.; Zheng, B.; Chen, J.; Zhuo, L.; Weng, Z.; Wang, Y.; Wang, H.; et al. Metal–organic–frameworks–isolated Au nanobipyramids as synergetic surface–enhanced–Raman–scattering substrates. *ACS Mater. Lett.* **2022**, *4*, 2506–2514. [CrossRef]
51. Wang, Q.; Xu, Z.; Zhao, Y.; Sun, H.; Bu, T.; Zhang, C.; Wang, X.; Wang, L. Bio–inspired self–cleaning carbon cloth based on flower–like Ag nanoparticles and leaf–like MOFs: A high–performance and reusable substrate for SERS detection of azo dyes in soft drinks. *Sens. Actuat. B–Chem.* **2021**, *329*, 129080. [CrossRef]
52. Xu, S.; Chen, P.; Lin, X.; Khan, I.; Ma, X.; Wang, Z. Controllable synthesis of flower–like AuNFs@ZIF–67 core–shell nanocomposites for ultrasensitive SERS detection of histamine in fish. *Anal. Chim. Acta* **2023**, *1240*, 340776. [CrossRef] [PubMed]
53. Xu, H.; Zhu, J.; Cheng, Y.; Cai, D. Functionalized UIO–66@Ag nanoparticles substrate for rapid and ultrasensitive SERS detection of di–(2–ethylhexyl) phthalate in plastics. *Sens. Actuat. B–Chem.* **2021**, *349*, 130793. [CrossRef]
54. Li, J.; Liu, Z.; Tian, D.; Li, B.; Shao, L.; Lou, Z. Assembly of gold nanorods functionalized by zirconium–based metal–organic frameworks for surface enhanced Raman scattering. *Nanoscale* **2022**, *14*, 5561–5568. [CrossRef]

55. Osterrieth, J.; Wright, D.; Noh, H.; Kung, C.; Vulpe, D.; Li, A.; Park, J.; Duyne, R.; Moghadam, P.; Baumberg, J.; et al. Core–shell gold nanorod@zirconium–based metal–organic framework composites as in situ size–selective Raman probes. *J. Am. Chem. Soc.* **2019**, *141*, 3893–3900. [CrossRef] [PubMed]
56. Zhao, X.; Yang, T.; Wang, D.; Zhang, N.; Yang, H.; Jing, X.; Niu, R.; Yang, Z.; Xie, Y.; Meng, L. Gold nanorods/metal–organic framework hybrids: Photo–enhanced peroxidase–like activity and SERS performance for organic dyestuff degradation and detection. *Anal. Chem.* **2022**, *94*, 4484–4494. [CrossRef]
57. Qin, Y.; Hao, M.; Wang, J.; Yuan, R.; Li, Z. Rational design of a core–shell structured plasmonic Au@MIL–100(Fe) nanocomposite for efficient photocatalysis. *ACS Appl. Mater. Interfaces* **2022**, *14*, 56930–56937. [CrossRef] [PubMed]
58. Xie, D.; Wang, R.; Fu, J.; Zhao, Z.; Li, M. AuNPs@MIL–101 (Cr) as a SERS–active substrate for sensitive detection of VOCs. *Front. Bioeng. Biotech.* **2022**, *10*, 921693. [CrossRef]
59. Hu, S.; Jiang, Y.; Wu, Y.; Guo, X.; Ying, Y.; Wen, Y.; Yang, H. Enzyme–free tandem reaction strategy for surface–enhanced Raman scattering detection of glucose by using the composite of Au nanoparticles and porphyrin–based metal–organic framework. *ACS Appl. Mater. Interfaces* **2020**, *12*, 55324–55330. [CrossRef]
60. Sun, Y.; Yu, X.; Hu, J.; Zhuang, X.; Wang, J.; Qiu, H.; Ren, H.; Zhang, S.; Zhang, Y.; Hu, Y. Constructing a highly sensitivity SERS sensor based on a magnetic metal–organic framework (MOFs) to detect the trace of thiabendazole in fruit juice. *ACS Sustain. Chem. Eng.* **2022**, *10*, 8400–8410. [CrossRef]
61. Shao, Q.; Zhang, D.; Wang, C.; Tang, Z.; Zou, M.; Yang, X.; Gong, H.; Yu, Z.; Jin, S.; Liang, P. Ag@MIL–101(Cr) film substrate with high SERS enhancement effect and uniformity. *J. Phys. Chem. C* **2021**, *125*, 7297–7304. [CrossRef]
62. Zhang, X.; Xie, X.; Zhang, L.; Yao, K.; Huang, Y. Optoplasmonic MOFs film for SERS detection. *Spectrochim. Acta A* **2022**, *278*, 121362. [CrossRef]
63. Kim, H.; Trinh, B.; Kim, K.; Moon, J.; Kang, H.; Jo, K.; Akter, R.; Jeong, J.; Lim, E.; Jung, J.; et al. Au@ZIF–8 SERS paper for food spoilage detection. *Biosens. Bioelectron.* **2021**, *179*, 113063. [CrossRef] [PubMed]
64. Yang, K.; Zong, S.; Zhang, Y.; Qian, Z.; Liu, Y.; Zhu, K.; Li, L.; Li, N.; Wang, Z.; Cui, Y. Array–assisted SERS microfluidic chips for highly sensitive and multiplex gas sensing. *ACS Appl. Mater. Interfaces* **2020**, *12*, 1395–1403. [CrossRef] [PubMed]
65. Oh, M.; De, R.; Yim, S. Highly sensitive VOC gas sensor employing deep cooling of SERS film. *J. Raman Spectrosc.* **2018**, *49*, 800–809. [CrossRef]
66. Alvarado, R.; Otero, N.; Mandado, M.; Berdullas, N. Simulating the Detection of Dioxin–like Pollutants with 2D Surface–Enhanced Raman Spectroscopy Using h–BNC Substrates. *Chemosensors* **2023**, *11*, 266. [CrossRef]
67. Chen, Q.; Hou, R.; Zhu, Y.; Wang, X.; Zhang, H.; Zhang, Y.; Zhang, L.; Tian, Z.; Li, J. Au@ZIF–8 core–shell nanoparticles as a SERS substrate for volatile organic compound gas detection. *Anal. Chem.* **2021**, *93*, 7188–7195. [CrossRef]
68. Xia, Z.; Li, D.; Deng, W. Identification and detection of volatile aldehydes as lung cancer biomarkers by vapor generation combined with paper–based thin–film microextraction. *Anal. Chem.* **2021**, *93*, 4924–4931. [CrossRef]
69. Lafuente, M.; Marchi, S.; Urbiztondo, M.; Pastoriza–Santos, I.; Pérez–Juste, I.; Santamaría, J.; Mallada, R.; Pina, M. Plasmonic MOFs thin films with Raman internal standard for fast and ultrasensitive SERS detection of chemical warfare agents in ambient air. *ACS Sens.* **2021**, *6*, 2241–2251. [CrossRef]
70. Dong, A.; Chen, D.; Li, Q.; Qian, J. Metal–organic frameworks for greenhouse gas applications. *Small* **2022**, *19*, 2201550. [CrossRef]
71. Huang, K.; Gong, S.; Zhang, L.; Zhang, H.; Li, S.; Ye, G.; Huang, F. Ultrathin ZIF–8 wrapping on Au–dotted Ag–nanowires for highly selective SERS–based CO_2 gas detection. *Chem. Commun.* **2021**, *57*, 2144–2147. [CrossRef]